A CORRELATION-BASED METHOD FOR DIRECTION FINDING OF MULTIPATH SIGNALS IN FREQUENCY HOPPING SYSTEMS

PENG NINGKUN

NATIONAL UNIVERSITY OF SINGAPORE

2004/2005

A CORRELATION-BASED METHOD FOR DIRECTION FINDING OF MULTIPATH SIGNALS IN FREQUENCY HOPPING SYSTEMS

PENG NINGKUN

(*M. Eng, Huazhong University of Science and Technology*)

A THESIS SUBMITTED

FOR THE DEGREE OF MASTER OF ENGINEERING

DEPARTMENT OF ELECTRICAL AND COMPUTER ENGINEERING

NATIONAL UNIVERSITY OF SINGAPORE

2004/2005

Acknowledgement

I would like to express my sincere thanks to my supervisors, Professor Ko Chi Chung, Dr. Zhi Wanjun and Dr. Francois Chin, for their invaluable guidance, support, encouragement, patience, advice and comments throughout my research work and this thesis.

Special thanks to my parents, my girlfriend and sister, who always encourage, support and care for me throughout my life.

I also wish to give my thanks to all students and staffs in Communications Lab at Department of Electrical and Computer Engineering for their helpful discussion and friendship.

I am grateful for research scholarship from the National University of Singapore for giving me the opportunity to carry out my research work.

Contents

List of Figures

List of Tables

Nomenclature

a	scalar
$\boldsymbol{a}$	column vector
$\mathbf{A}$	Matrix
$\mathbf{A}^{+}$	Pseudo-inverse of Matrix
$[\bullet]^{T}$	Transpose of matrix or vector
$[\bullet]^{H}$	Hermitian transpose
$[\bullet]^{-1}$	Matrix inversion
$\nabla_x f(x)$	The gradient of $f(x)$ with respect to x
FSK	Frequency Shift Keying
PSK	Phase Shift Keying

Summary

Direction finding is of great interest in many applications such as GPS (Global Positioning System), radar, sonar and wireless communication systems. In smart antenna systems, the direction of users is an important factor to increase the capacity, and an antenna array is usually used at the base station to estimate and track the direction of users.

Conventional direction finding methods solve the problem of direction-of-arrival (DOA) estimation for narrowband signals, and usually these methods require that the number of array elements be larger than the number of signal sources. In military communications and some short-range wireless communication systems (e.g. Bluetooth), frequency hopping technique is widely used. In such systems, it is difficult to equip a large size antenna array. Therefore, it is necessary to solve the direction finding problem for the frequency hopping systems by using an antenna array with a lesser number of elements.

In this thesis, a new method is proposed to estimate and track the directions of frequency hopping signals under multipath propagation. Only the power of transmitted signal is needed to be known in this method. With a two-element array at the receiver, the objective function is established by minimizing the differece between the estimated correlations and the measured correlations of the received signals. The

Gauss-Newton algorithm is utilized to find the optimum parameters including directions. Compared with an existing method, the proposed method has more accurate converged results. Additionally, the new method is easy to implement as analog devices can be used to measure the correlations of received signals.

Future work can be carried out to reduce the computational complexity by decreasing the number of unknown parameters. Further analysis can be done in the tracking scenario if more parameters vary with respect to time or hops.

Chapter 1

Introduction

Direction finding is of great research interest for decades. It has been widely used in many applications such as sonar, radar and communication systems. With the rapid development of wireless communication, smart antenna is an important research area due to the fast increasing number of users and the requirement on high bit rate data service. To provide enough capacity, the position information of users is a crucial factor for smart antenna systems [1], which is quite different from former wireless communication systems. Hence, the algorithms for direction finding and source localization need to be more computationally efficient as the number of users increases. Many different scenarios should also be considered.

1.1 Evolution of Wireless Communication Systems

Wireless communication has been developed for many years. Before 1960s, mobile users communicated with each other by amplitude modulation (AM) or frequency modulation (FM) radio which cannot connect to the public switched telephone network (PSTN). In 1960s and 1970s, Bell Laboratories developed the cellular concept which makes the wide use of wireless communication become possible. The first generation of mobile communication systems is analog system that is widely

used in 1980s such as European Total Access Cellular System (ETACS) and Advanced Mobile Phone System (AMPS) in North America [2]. These two systems use frequency division multiple access (FDMA) to maximize capacity.

In 1990s, the digital system GSM (Global System for Mobile) was deployed to replace ETACS system in Europe and it is accepted worldwide except North America and Japan which developed USDC (U.S. Digital Cellular) and PDC (Pacific Digital Cellular) systems respectively [2]. One of the common features of these systems is that TDMA (Time Division Multiple Access) is used in place of analog FDMA. Given the application of digital signal processing and speech coding technology, the second generation mobile communication systems have better voice quality and larger capacity than analog systems.

In 1993, Qualcomm Inc developed a cellular system based on code division multiple access (CDMA) [2]. This is the start of the third generation mobile communication systems. CDMA systems have better interference resistance, larger capacity and are more power efficient than former systems. Furthermore, it also can provide high bit rate data service to satisfy the increasing requirements on wireless broadband access service.

Direction estimation is of importance in these communication systems. For example, in a cellular mobile system, the inter-user interference degrades the performance severely. Using an antenna array at the base station will solve this problem. The receiving array can be steered in the direction of one user at a time, while

nulling interference from other users at the same time [8]. This is indeed one of the motivations of smart antenna technology.

1.2 Introduction to Smart Antenna Technology

The purpose for developing smart antenna technology is to meet the capacity demands of cellular mobile system. In traditional systems, users communicating through the same base station are separated by frequency (FDMA), by time (TDMA), or by code (CDMA), while smart antennas add a new way, by space, which make users in the same cell communicate with base station via the same physical channel. Therefore the capacity of smart antenna systems is much larger than that of traditional technologies. Another improvement is that the power consumption in smart antenna systems is much lower [1]. In GSM and CDMA systems, base station antennas are omnidirectional or sectored. Therefore, some of the power is wasted as it is radiated to other directions than to the desired users, and it also will be experienced as interference by other users. The antenna patterns of smart antennas are not fixed but can adapt to the current situation by maximizing the antenna gain in the desired direction and minimizing the radiation pattern in the interference direction at the same time. Thus the interference from other users is significantly reduced to the desired user and the base station is more power efficient. It also should be noted that the smart antenna system not only includes the radiating elements but also consists of a combining/dividing network and a control unit. The control unit implements the intelli-

gence of smart antennas.

Smart antenna technology is not fully commercially available now. In practice, it has been in testbeds already. Ericsson built a test system for smart antenna base stations in 1998. Another test system is Tsunami II, a project of the European 4th framework program. And a smart antenna base station is built to perform trials in different environments. Similar works have also been carried out in other countries including U.S. [3], Canada, Japan [4] and Korea [5].

1.3 Direction Finding and Source Localization

A number of position location systems have been developed over years. Among these systems, Global Positioning System (GPS) is the most popular radio navigation system for its worldwide availability, high accuracy and low cost. The theory of GPS is easy to understand. The satellites are equipped with highly precise clocks and the signal transmitted from satellites contains the clock information. An accurate clock at the receiver measures the time delay between the signals leaving the satellites and arriving at the receiver. If the signals of three satellites are available, the coordinates (latitude, longitude and altitude) of the receiver are easy to calculate via triangulation [6].

Another important source localization method uses the cellular mobile system instead of satellite system to estimate the position of mobile terminals. The idea is

similar to the theory of GPS. The signal transmitted by the mobile terminal is received by multiple base stations, and the position of mobile can be determined by DOA (Direction of Arrival) or TDOA (Time Difference of Arrival) estimation methods. The difference between localization in the cellular mobile system and GPS is that the GPS receiver calculates the coordinates itself by using the received data from the satellites, but it is the base stations to compute the position of the mobile in the cellular mobile localization [7]. Compared with GPS, localization in cellular mobile system can be implemented at the base stations, which makes the standard mobile terminal be tracked without extra costs for consumers. Another advantage of cellular localization is that the mobile service providers can determine the capacity needs of a particular area so that they can adjust the networks accordingly.

1.4 Source Localization using DOA, TOA and TDOA

In the cellular mobile systems, the source localization can be accomplished by DOA, TOA (time of arrival) and TDOA estimation methods. To do position location via DOA estimation, at least two base stations are needed for 2-dimensional localization. The position of the mobile can be found at the intersection of the two lines as shown in Fig. 1.1. In Fig. 1.1, A and B are two base stations and P is the mobile. If the base stations can estimate the direction of the signal from mobile P, it is easy to see that the position of the mobile is the intersection of AP and BP.

The source localization via TOA method requires at least three base stations for 3-dimensional positioning. Because the electromagnetic waves have a constant propagation speed (normally it is the speed of light), the distances d_1, d_2, d_3 between the mobile target and the three base stations can be calculated given the estimation of the TOAs. The mobile must lie on a sphere of radius d_i from the corresponding base station. Thus the position of the mobile is the intersection of these three circles. However, the TOA method imposes a rigorous requirement for the clock synchronization (e.g., $1\mu s$ timing error would result in $300m$ position error), and it requires the transmitting signal contains time information as well. Thus TDOA method is more commonly used instead of TOA method.

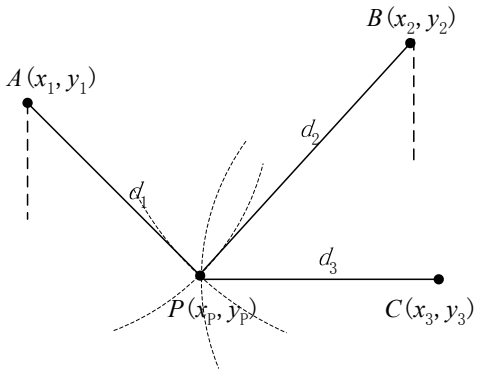

Fig. 1.1 Localization via DOA in two-dimension.

TDOA is the time difference at which the signal arrives at multiple base stations. For example, if the transmitted signal of the mobile arrives at two base stations at t_1 and t_2, respectively, the TDOA is $t_2 - t_1$. If the TDOA has been measured, the mobile target should lie on a hyperbola (for 2-dimension) or hyperboloid (for 3-dimension) whose foci are the locations of the base stations. Thus, the position of the mobile is determined by the unique intersection of these hyperbolas.

1.5 Organization of the Thesis

In this thesis, we concentrate on the direction estimation problem for frequency hopping signals, and a new method is proposed to track multipath frequency hopping signals.

In Chapter 2, several popular methods for DOA estimation are addressed including maximum likelihood methods, subspace methods and beamforming techniques. The model of frequency hopped signals under multipath propagation is discussed as well.

The objective function of the proposed method is derived in Chapter 3. Several searching methods are studied including steepest descent method, Newton's method, Gauss-Newton method and alternating minimization method. At the end of this chapter, the detailed algorithm is proposed to solve the objective function of our method.

In Chapter 4, simulation is performed for the new method in both stationary and slow moving scenario. To enable the comparison with another method-the FHML (Frequency Hopping Maximum Likelihood) method, Monte-Carlo experiments are done for both methods in the same scenario.

Finally, conclusions are drawn in Chapter 5 based on the analysis in preceding

chapters. Further extensions of this research work are suggested.

Chapter 2

Direction Estimation using Antenna Array

2.1 Introduction to DOA Estimation Methods

In the previous chapter, we have introduced several source localization methods using DOA, TOA and TDOA. The direction parameters are usually estimated with an antenna array which has a certain geometric shape, and the estimation task is performed by exploiting the data collected at different sensors. The uniform linear array (ULA) and the uniform circular array (UCA) are the most regularly used, and they have been proven useful for the source localization in sonar, radar [8] and mobile communications [27][28].

In this chapter, the signal model is introduced first. Then several classical methods are discussed including spectral-based methods and the maximum likelihood (ML) methods. The spectral-based methods include beamforming techniques and subspace methods. In these methods, some spectrum-like functions of the parameter of interests are formed and the location of the highest peaks of the function is the result of the estimation task. In the ML methods, usually a brute force search is used to find the optimum parameters. Compared with spectral-based methods, the ML methods are more computationally expensive but the results of ML methods are more accurate.

2.2 Signal Model for DOA Estimation

Before we introduce the signal model, some assumptions are made as follows.

a) The spacing of adjacent antennas is small enough so that there is no amplitude difference between the received signals at contiguous antennas.

b) The signal of interests is a narrowband signal, which means the bandwidth of the signal is much smaller than the carrier frequency.

c) There is no mutual coupling effect between array elements.

d) The transmitter is a far-field source and the transmitted signal is plane wave when it arrives at the receiving array [8].

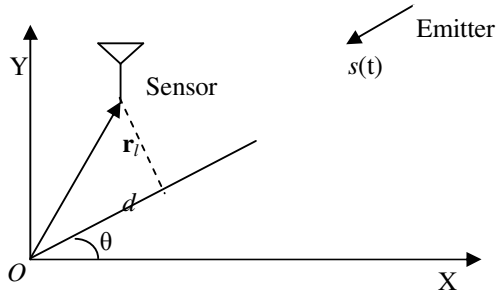

Fig. 2.1 Two-dimensional array geometry.

In Fig. 2.1, the transmitted signal $s(t)$ arrives at the sensor with angle-of-arrival θ. The coordinates vector of the sensor is $\mathbf{r}_l = (x_l, y_l)^{\mathrm{T}}$. The origin O is taken as the reference and the signal at the origin O is

$$E(0,t) = s(t)e^{j\omega_c t} \tag{2.1}$$

where $f_c = \omega_c / 2\pi$ is the carrier frequency.

Thus, the received signal at the sensor is

$$E(\mathbf{r}_l, t) = s(t)e^{j[\omega_c t - k(x_l \cos\theta + y_l \sin\theta)]} \tag{2.2}$$

where $k = 2\pi / \lambda$ is the wave number, and λ is the wavelength.

Equation (2.2) is obviously true because the wave arrives at the sensor earlier than it arrives at the origin by a distance *d*, where $d = x_l \cos\theta + y_l \sin\theta$. Thus, the phase of the signal at the sensor is $k(x_l \cos\theta + y_l \sin\theta)$ earlier than the phase at the origin. Furthermore, if a flat frequency response, say $g_l(\theta)$, is assumed for the sensor over the bandwidth, the measured output should be multiplied by a gain (or attenuation) factor $g_l(\theta)$ [8]. Then (2.2) becomes

$$x_l(t) = s(t) g_l(\theta) e^{j[\omega_c t - k(x_l \cos\theta + y_l \sin\theta)]} = a_l(\theta) s(t) \tag{2.3}$$

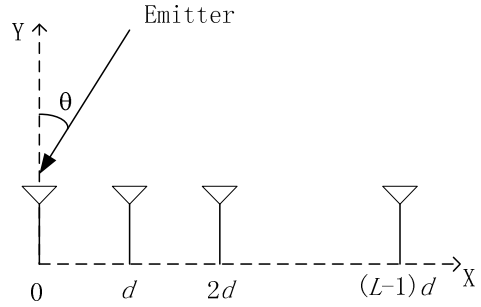

Fig. 2.2 ULA array geometry.

For a ULA array as Fig. 2.2 shows, the model of received signal can be derived similarly. Assume that all array elements have the same frequency response, i.e. $g_0(\theta) = g_1(\theta) = ... = g_{L-1}(\theta) = g(\theta)$ and the element 0 is taken as the reference. The array output is

$$\mathbf{x}(t) = \mathbf{a}(\theta) s(t) \tag{2.4}$$

where $\mathbf{x}(t) = [x_0(t) \quad x_2(t) \quad ... \quad x_{L-1}(t)]^{\mathrm{T}}$, *d* is the distance between two adjacent array elements, and

$$\mathbf{a}(\theta) = g(\theta)\left[1 \quad e^{-jkd\sin\theta} \quad ... \quad e^{-j(L-1)kd\sin\theta}\right]^{\mathrm{T}}. \tag{2.5}$$

The DOA defined in (2.4) is the clockwise angle from Y axis to the direction of signal propagation. The vector $\mathbf{a}(\theta)$ is named steering vector (or array propagation vector, action vector). In (2.4), only one source is considered. If there are more than one source, (2.4) becomes

$$\mathbf{x}(t) = \sum_{m=1}^{M} \mathbf{a}(\theta_m) s_m(t) \tag{2.6}$$

where M is the number of sources or paths. To write (2.6) in a compact form, we can define a steering matrix and a vector of signal as follows

$$\mathbf{A}(\boldsymbol{\theta}) = [\mathbf{a}(\theta_1) \quad \mathbf{a}(\theta_2) \quad ... \quad \mathbf{a}(\theta_M)] \tag{2.7}$$

$$\mathbf{s}(t) = [s_1(t) \quad s_2(t) \quad ... \quad s_M(t)]^{\mathrm{T}} . \tag{2.8}$$

If additive noise is added at the array elements, the commonly used model can be shown as follows

$$\mathbf{x}(t) = \mathbf{A}(\boldsymbol{\theta})\mathbf{s}(t) + \mathbf{n}(t) . \tag{2.9}$$

We also assume that the number of signal sources is less than the number of antenna elements throughout this thesis, i.e. $M<L$. Now, we have derived the signal model for the DOA estimation and array processing.

2.3 Signal Model under Multipath Propagation

When signal is propagated over a multipath channel, the received signal will be a superposition of several replica of the transmitted signal with different time delay.

Suppose the transmitted signal is

$$s(t) = \mathrm{Re}\left[s_l(t)e^{j2\pi f_c t}\right] \tag{2.10}$$

where $s_l(t)$ is the baseband signal, f_c is carrier frequency. The signal passes through multiple paths, each with a propagation delay and an attenuation factor. The delay and the attenuation factor may vary with time, which is dependent on the propagation medium [9]. So the received signal should be

$$x(t) = \sum_n \alpha_n(t)s[t - \tau_n(t)] \tag{2.11}$$

where $\alpha_n(t)$ and $\tau_n(t)$ are the channel attenuation factor and the propagation time delay with respect to *n*th path respectively. Substituting (2.10) into (2.11), the received signal becomes

$$x(t) = \mathrm{Re}\left(\left\{\sum_n \alpha_n(t)e^{-j2\pi f_c \tau_n(t)} s_l[t - \tau_n(t)]\right\} e^{j2\pi f_c t}\right). \tag{2.12}$$

From (2.12), we can see that the baseband part of the received signal is

$$r_l(t) = \sum_n \alpha_n(t)e^{-j2\pi f_c \tau_n(t)} s_l[t - \tau_n(t)]. \tag{2.13}$$

So the channel impulse response can be described as follows

$$c(\tau; t) = \sum_n \alpha_n(t)e^{-j2\pi f_c \tau_n(t)} \delta[\tau - \tau_n(t)]. \tag{2.14}$$

It also should be noted that all derivations above are based on discrete multipath channel. In this thesis, the continuous case is not considered.

The multipath channel will cause the fading problem. Suppose $s_l(t) = 1$ for all *t* in previous equations, the received signal is given by

$$r_l(t) = \sum_n \alpha_n(t)e^{-j2\pi f_c \tau_n(t)} = \sum_n \alpha_n(t)e^{-j\theta_n(t)}. \tag{2.14}$$

Since $\theta_n(t)$ varies quickly, the received signal may be very small when the vectors $\alpha_n(t)e^{-j\theta_n(t)}$ are adding destructively. At other times the received signal $r_l(t)$ may be large when the vectors $\alpha_n(t)e^{-j\theta_n(t)}$ are adding constructively. So the amplitude of received signal may vary quickly, which terms signal fading.

2.4 Introduction to Frequency Hopping Systems

Frequency hopping (FH) is one of the spread spectrum techniques. In a FH system, the channel bandwidth is divided into a sequence of frequency slots. The transmitted signal may occupy one or more of the frequency slots for a signal symbol. Usually, the frequency slots for each signal symbol are selected pseudorandomly according to the output of a PN generator [9].

Assume $p(t)$ is a basic pulse shape of duration T_h (hop time), frequency modulation has the form

$$c(t) = \sum_n \mathrm{Re}\left[e^{j(2\pi f_n t + \phi_n)} p(t - nT_h)\right] \tag{2.16}$$

where f_n is pseudorandomly generated sequence and ϕ_n is the byproduct of the modulation process.

At the receiver, usually there is also an identical PN generator which is synchronized with the one at the transmitter. It is used to remove the psedorandom frequency introduced in the transmitter. For the modulation techniques, FSK is more often used although the performance of FSK is not better than that of PSK in additive

white Gaussian noise (AWGN) channel. This is because it is difficult to maintain phase coherence of the hopping frequencies as the frequency of transmitted signal is hopped from one to another over a wide band channel.

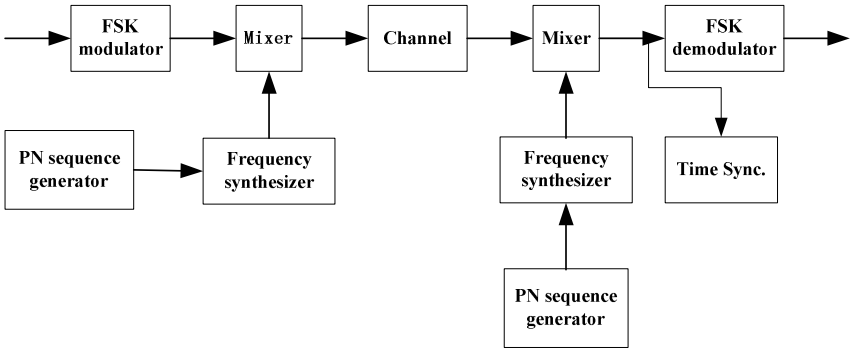

Fig. 2.3 Block diagram of a FH spread spectrum system

The FH rate is usually selected to be either equal to the symbol rate or faster than symbol rate. If there are multiple hops for one symbol duration, it is called fast frequency hopping (FFH) signal. On the other hand, if the hopping rate is equal to or slower than the symbol rate, it is called slow frequency hopping (SFH) signal. In this thesis, only SFH signal is considered.

2.5 DOA Estimation Methods

Before introducing the classic methods, the statistics of the received signal should be checked. When a ULA is used, the covariance matrix of the received signal is

$$\mathbf{R} = \mathrm{E}\{\mathbf{x}(t)\mathbf{x}^H(t)\} = \mathbf{A}\mathrm{E}\{\mathbf{s}(t)\mathbf{s}^H(t)\}\mathbf{A}^H + \mathrm{E}\{\mathbf{n}(t)\mathbf{n}^H(t)\} \tag{2.17}$$

where $\mathbf{A}(\boldsymbol{\theta}) = [\mathbf{a}(\theta_1) \quad \mathbf{a}(\theta_2) \quad \ldots \quad \mathbf{a}(\theta_M)]$ is defined in (2.7).

The source signal covariance matrix is

$$\mathbf{P} = \mathrm{E}\{\mathbf{s}(t)\mathbf{s}^H(t)\} \tag{2.18}$$

and the noise covariance matrix is

$$\mathrm{E}\{\mathbf{n}(t)\mathbf{n}^H(t)\} = \sigma^2\mathbf{I}. \tag{2.19}$$

Here, we assume the noises at all sensors have a common variance σ^2 and are mutually independent, also we assume that the mean of noise vector $\mathbf{n}(t)$ is zero. This is usually called spatially white. Furthermore, the source covariance matrix is often assumed to be nonsingular (it may be singular in the case of coherent signal) or near singular for highly correlated signal.

The spectral factorization of the covariance matrix of received signal is very important, and it can be in the following representation

$$\mathbf{R} = \mathbf{APA}^H + \sigma^2\mathbf{I} = \mathbf{U\Lambda}\cdot\mathbf{U}^H \tag{2.20}$$

where $\mathbf{U}$ is a unitary matrix and $\mathbf{\Lambda} = \mathrm{diag}\{\lambda_1 \quad \lambda_2 \quad ... \quad \lambda_L\}$ is a diagonal matrix of eigenvalues and we assume that $\lambda_1 \geq \lambda_2 \geq ... \geq \lambda_L > 0$.

It is noted that any column vector orthogonal to the columns of matrix $\mathbf{A}$ is an eigenvector of $\mathbf{R}$ with eigenvalue σ^2. This is easy to show. Assume vector $\mathbf{q}$ is orthogonal to $\mathbf{A}$. Thus, right multiply (2.20) at both sides by $\mathbf{q}$, we have $\mathbf{Rq} = \left(\mathbf{APA}^H + \sigma^2\mathbf{I}\right)\mathbf{q} = \sigma^2\mathbf{q}$. Obviously $\mathbf{q}$ is an eigenvector of $\mathbf{R}$ with eigenvalue σ^2. Also there are $L-M$ linearly independent such vectors. The rest of the eigenvalues are larger than σ^2. So we can partition the eigenvectors into two groups- noise eigenvectors (corresponding to eigenvalues equal to σ^2) and signal eigenvectors (corresponding to eigenvalues larger than σ^2). Hence, (2.20) becomes

$$\mathbf{R} = \mathbf{U}_s \mathbf{\Lambda}_s \mathbf{U}_s{}^H + \mathbf{U}_n \mathbf{\Lambda}_n \mathbf{U}_n{}^H \tag{2.21}$$

where $\mathbf{\Lambda}_n = \sigma^2 \mathbf{I}_n$, and the dimension of $\mathbf{I}_n$ is $L - M$. Because all noise eigenvectors are orthogonal to **A**, the columns of $\mathbf{U}_s$ must span the range space of **A** and those of $\mathbf{U}_n$ span its orthogonal complement. The projection operators of these signal and noise subspaces are

$$\mathbf{\Pi} = \mathbf{U}_s \mathbf{U}_s{}^H = \mathbf{A}\left(\mathbf{A}^H \mathbf{A}\right)^{-1} \mathbf{A}^H \tag{2.22}$$

$$\mathbf{\Pi}^{\perp} = \mathbf{U}_n \mathbf{U}_n{}^H = \mathbf{I}_s - \mathbf{A}\left(\mathbf{A}^H \mathbf{A}\right)^{-1} \mathbf{A}^H . \tag{2.23}$$

where the dimension of $\mathbf{I}_s$ is M.

Now, we have a receiving array to receive emitter signals and use these signals to estimate the DOA parameters. The received signal is given as a finite data set $\{\mathbf{x}(t)\}$ sampled at $t = 1,2,...,N$. In the previous formulations, the statistical expectation of $\mathbf{x}(t)$ is used, which requires infinite data samples. In practice, equation below is used to replace the expectation

$$\hat{\mathbf{R}} = \frac{1}{N} \sum_{t=1}^{N} \mathbf{x}(t) \mathbf{x}^H(t) . \tag{2.24}$$

Similarly (2.24) becomes

$$\hat{\mathbf{R}} = \hat{\mathbf{U}}_s \hat{\mathbf{\Lambda}}_s \hat{\mathbf{U}}_s{}^H + \hat{\mathbf{U}}_n \hat{\mathbf{\Lambda}}_n \hat{\mathbf{U}}_n{}^H . \tag{2.25}$$

In this thesis, those equations introduced above are important and will be frequently used. We will introduce the beamforming technique first.

2.5.1 Beamforming Techniques

The idea behind beamforming method is that the estimated DOA (if it is correct) will result in maximum output power given a series of observed data [8]. The array output is

$$y(t) = \sum_{l=1}^{L} w_l^{*} x_l(t) = \mathbf{w}^H \mathbf{x}(t). \tag{2.26}$$

Given the observed data, the output power is

$$P(\mathbf{w}) = \frac{1}{N}\sum_{l=1}^{N} |y(t)|^2 = \frac{1}{N}\sum_{l=1}^{N} \mathbf{w}^H \mathbf{x}(t)\mathbf{x}^H(t)\mathbf{w} = \mathbf{w}^H \hat{\mathbf{R}} \mathbf{w} \tag{2.27}$$

where $\hat{\mathbf{R}}$ is defined in (2.24). Since $\mathbf{x}(t) = \mathbf{a}(\boldsymbol{\theta})s(t) + \mathbf{n}(t)$, we have

$$\begin{aligned} \max_{\mathbf{w}} \mathrm{E}\{\mathbf{w}^H \mathbf{x}(t)\mathbf{x}^H(t)\mathbf{w}\} &= \max_{\mathbf{w}} \mathbf{w}^H \mathrm{E}\{\mathbf{x}(t)\mathbf{x}^H(t)\}\mathbf{w} \\ &= \max_{\mathbf{w}} \{\mathrm{E}|s(t)|^2 |\mathbf{w}^H \mathbf{a}(\boldsymbol{\theta})|^2 + \sigma^2 |\mathbf{w}|^2\} \end{aligned} \tag{2.28}$$

Here, we assume that the additive noise is white. Another assumption is that the norm of $\mathbf{w}$ is constrained to $|\mathbf{w}| = 1$. Thus we can find the result of $\mathbf{w}$

$$\mathbf{w}_{BF} = \frac{\mathbf{a}(\boldsymbol{\theta})}{\sqrt{\mathbf{a}^H(\boldsymbol{\theta})\mathbf{a}(\boldsymbol{\theta})}} \tag{2.29}$$

Substituting (2.29) into (2.27), the spatial spectrum of the beamforming technique is obtained

$$P_{BF}(\boldsymbol{\theta}) = \frac{\mathbf{a}^H(\boldsymbol{\theta})\hat{\mathbf{R}}\mathbf{a}(\boldsymbol{\theta})}{\mathbf{a}^H(\boldsymbol{\theta})\mathbf{a}(\boldsymbol{\theta})}. \tag{2.30}$$

The steering vector $\mathbf{a}(\boldsymbol{\theta})$ takes the form

$$\mathbf{a}(\boldsymbol{\theta}) = \begin{bmatrix} 1 & e^{j\phi} & \ldots & e^{j(L-1)\phi} \end{bmatrix} \tag{2.31}$$

where

$$\phi = -kd\sin\theta = -\frac{\omega}{c}d\sin\theta\,. \tag{2.32}$$

Thus the DOA can be estimated by finding the peaks of $P_{BF}(\boldsymbol{\theta})$.

The drawback of beamforming technique is that the resolution is highly dependent on the array structure. It cannot distinguish two closely spaced sources no matter how many observed data samples are used. Usually the angles of arrival should have at least $2\pi / L$ difference (in radian, L is the distance between two adjacent antennas).

To ease the resolution limitation of the above beamformer, an improved beamformer was proposed by Capon [8]. The optimization problem is re-formulated as follows

$$\min_{\mathbf{w}} P(\mathbf{w}) \tag{2.33}$$

subject to

$$\mathbf{w}^H\mathbf{a}(\boldsymbol{\theta}) = 1. \tag{2.34}$$

where $P(\mathbf{w})$ is defined in (2.27).

The Capon's method attempts to minimize the power contributed by noise and signal coming from other angles, while a fixed power is maintained in the direction $\boldsymbol{\theta}$. The optimal $\mathbf{w}$ can be found using Lagrange multipliers, and it is as follows

$$\mathbf{w}_{CAP} = \frac{\hat{\mathbf{R}}^{-1}\mathbf{a}(\boldsymbol{\theta})}{\mathbf{a}^H(\boldsymbol{\theta})\hat{\mathbf{R}}^{-1}\mathbf{a}(\boldsymbol{\theta})}. \tag{2.33}$$

Substituting (2.33) into (2.31), we obtain following spatial spectrum

$$P_{CAP}(\boldsymbol{\theta}) = \frac{1}{\mathbf{a}^H(\boldsymbol{\theta})\hat{\mathbf{R}}^{-1}\mathbf{a}(\boldsymbol{\theta})}. \tag{2.34}$$

The Capon's method exploits every degree of freedom to concentrate the received energy along one direction as shown by the constraint condition. So it has a better resolution than conventional beamforming technique. It also can be interpreted as the Capon's method is more focused on minimizing the power in the directions where there are sources other than desired one. This method is computationally easy to implement because only the autocorrelation matrix is needed to be estimated to evaluate the spectral density. However, the Capon's method is still dependent on the array aperture and the signal to noise ratio (SNR) [8].

2.5.2 Subspace Methods

Now we will introduce subspace methods. The subspace methods exploit the eigen-structure of the covariance matrix of received signal. One of the most famous subspace methods is the MUSIC (Multiple Signal Classification) algorithm [10].

In the previous content, we noted that the structure of the covariance matrix of the received signal with white noise assumption implies such spectral decomposition as below

$$\hat{\mathbf{R}} = \mathbf{A}\mathbf{P}\mathbf{A}^H + \sigma^2\mathbf{I} = \mathbf{U}_s\boldsymbol{\Lambda}_s\mathbf{U}_s{}^H + \sigma^2\mathbf{U}_n\mathbf{U}_n{}^H \tag{2.37}$$

Here we assume $\mathbf{A}\mathbf{P}\mathbf{A}^H$ is of full rank, so the diagonal matrix $\boldsymbol{\Lambda}_s$ contains the M largest eigenvalues whose eigenvectors span a signal space. Because the eigenvec-

tors in $\mathbf{U}_n$ are orthogonal to **A**, we will have

$$\mathbf{U}_n{}^H \mathbf{a}(\theta) = 0, \quad \theta \in \{\theta_1,...,\theta_M\} \tag{2.38}$$

To obtain unique DOA estimates, the receiving array is usually assumed to be unambiguous, which implies that any collection of *L* steering vectors corresponding to distinct DOA θ_k forms a linearly independent set $\{a(\theta_1),...,a(\theta_L)\}$ (because $M < L$). Thus $\mathbf{APA}^H$ is of full rank if the source covariance matrix **P** has full rank. Then $\theta_1,...,\theta_M$ are the only possible solutions to the relation.

In practice, we use $\hat{\mathbf{R}} = \frac{1}{N}\sum_{t=1}^{N} \mathbf{x}(t)\mathbf{x}^H(t)$ instead of the statistical expectation of source covariance matrix. The eigenvectors are separated into the signal and the noise eigenvectors. The orthogonal projector onto the noise subspace is estimated as

$$\hat{\Pi}^{\perp} = \hat{\mathbf{U}}_n \hat{\mathbf{U}}_n{}^H \tag{2.39}$$

The objective function of MUSIC is

$$P_M(\boldsymbol{\theta}) = \frac{\mathbf{a}^H(\boldsymbol{\theta})\mathbf{a}(\boldsymbol{\theta})}{\mathbf{a}^H(\boldsymbol{\theta})\hat{\Pi}^{\perp}\mathbf{a}(\boldsymbol{\theta})} \tag{2.40}$$

Equation (2.40) will have peaks around the true DOAs as (2.38) implies. The performance improvement of the MUSIC method was so significant that it replaced most preceding methods. Particularly, the accuracy of estimation can be very high for this method if the data collection is sufficiently large or SNR is high enough and the signal model is adequately accurate. Thus the MUSIC algorithm has statistically consistent estimates (consistency means the estimates converges to the true value when the number of data tends to infinity) compared with the beamforming tech-

niques. However, the MUSIC method still has its limitations that it is difficult to distinguish closely spaced sources in small samples and in low SNR scenarios. And the MUSIC method also does not perform well for highly correlated signals. For the case of coherent signals (two signals are coherent if one is a scaled and delayed version of the other), the covariance matrix will no longer be of full rank and the MUSIC method fails to result in consistent estimates [11].

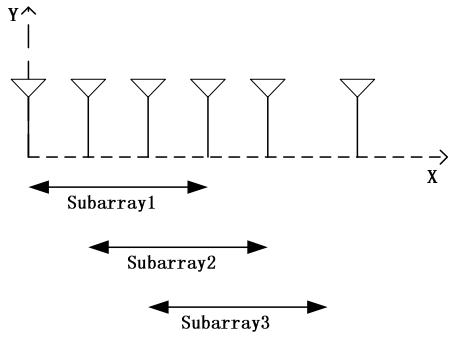

Fig. 2.4 Subarray structure for spatial smoothing technique.

To solve the problem of DOA estimation for coherent signals, some methods are developed to de-correlate the signals. One spatial smoothing method [12] proposed by Shan *et al* is based on averaging of the covariance matrix of identical overlapping arrays. This method needs the array elements have a periodic structure, such as ULA. Let a ULA with L identical array elements be divided into overlapping forward sub-arrays of size q as shown in Fig. 2.5. The kth forward sub-array is formed by $\{k,...,q+k-1\}$ array elements, where $k=\{1,2,...,L-q+1\}$. Then the signal received by the kth sub-arrays is

$$\mathbf{x}_k^f(t) = \mathbf{A}\mathbf{F}^{(k-1)}\mathbf{s}(t) + \mathbf{n}(t) \tag{2.41}$$

where $\mathbf{F}^{(k-1)}$ is the (k-1)th power of the diagonal matrix

$$\mathbf{F} = \begin{pmatrix} e^{j\phi_1} & 0 & \dots & 0 \\ 0 & e^{j\phi_2} & \dots & 0 \\ \dots & \dots & \dots & \dots \\ 0 & 0 & \dots & e^{j\phi_{M-1}} \end{pmatrix} \tag{2.42}$$

where $\phi_i = 2\pi f \dfrac{d\sin\theta_i}{c}$.

Thus the covariance matrix of the kth forward sub-arrays is

$$\mathbf{R}_k^f = \mathbf{A}\mathbf{F}^{(k-1)}\mathbf{R}_s\left(\mathbf{F}^{(k-1)}\right)^H \mathbf{A}^H + \sigma^2\mathbf{I} \tag{2.43}$$

Combining all subarrays' covariance matrices, a forward averaged spatially smoothed covariance matrix $\mathbf{R}^f$ is obtained

$$\begin{aligned} \mathbf{R}^f &= \frac{1}{L-q+1}\sum_{k=1}^{L-q+1}\mathbf{R}_k^f \\ &= \mathbf{A}\left(\frac{1}{L-q+1}\sum_{k=1}^{L-q+1}\mathbf{F}^{(k-1)}\mathbf{R}_s\left(\mathbf{F}^{(k-1)}\right)^H\right)\mathbf{A}^H + \sigma^2\mathbf{I} \\ &= \mathbf{A}\mathbf{R}_s^f\mathbf{A}^H + \sigma^2\mathbf{I} \end{aligned} \tag{2.44}$$

where

$$\mathbf{R}_s^f = \frac{1}{L-q+1}\sum_{k=1}^{L-q+1}\mathbf{F}^{(k-1)}\mathbf{R}_s\left(\mathbf{F}^{(k-1)}\right)^H. \tag{2.45}$$

For $L-q+1 \geq M$, the covariance matrix $\mathbf{R}_s^f$ will be nonsingular even if the received signals are coherent. Then conventional MUSIC method can be applied to find the DOA. If there are M DOAs to estimate, the number of subarrays should be more than $M+1$. Thus the number of array elements should be more than 2M. The spatial smoothing method has the similar computational efficiency of one-dimensional search. A backward averaged spatially smooth method can be de-

veloped similarly and it can be combined with forward averaged spatial smoothing to reduce the requirements on the number of array elements. We also should note that the spatial smoothing techniques need a ULA. If more general arrays are used, some sort of transformation should be done to the received signals. And the transformation may require some a priori knowledge of signal sources [8].

2.5.3 Maximum Likelihood (ML) Method

To estimate directions of highly correlated or coherent signals, parametric array signal processing methods are developed, which can more fully exploit the data model. ML methods can solve the problem of direction finding for coherent signals but they always need a multidimensional search to find the estimates as the tradeoff for increased efficiency and robustness. Here we still use ULA as the receiving array.

In the data model (2.9), we assumed that the additive noise is a stationary Gaussian white random process. If the signal is deterministic, for an observation $\mathbf{x}$ which is the function of the signal and noise parameter $\mathbf{\Theta}$, the joint probability distribution function of $\mathbf{x}$ can be regarded as a function of noise vector $\mathbf{\Theta}$. Let us use $l(\mathbf{\Theta})$ to denote the probability density function and it is also called the likelihood function. Since the noise is a white Gaussian process with σ^2 variance, the received signal is also a white Gaussian process with mean value of $\mathbf{A}(\boldsymbol{\theta})\mathbf{s}(t)$ and σ^2 variance. So the likelihood function can be shown to be

$$l(\mathbf{\Theta}) = \frac{1}{\left(\sqrt{2\pi\sigma^2}\right)^{LN}} e^{-\frac{\sum_{t=1}^{N} \|\mathbf{x}(t)-\mathbf{A}(\boldsymbol{\theta})\mathbf{s}(t)\|^2}{2\sigma^2}} \tag{2.46}$$

For convenience, the likelihood function is usually replaced by the log-likelihood function, which is given by

$$L(\boldsymbol{\Theta}) = -NL\ln\sigma - \frac{\sum_{t=1}^{N}\left\|\mathbf{x}(t)-\mathbf{A}(\boldsymbol{\theta})\mathbf{s}(t)\right\|^2}{2\sigma^2} \tag{2.47}$$

In (2.47), some parameter-independent terms are ignored. To compute the ML estimator, the log-likelihood function is maximized with respect to the unknown parameters. Fixing $\boldsymbol{\theta}$ and $\mathbf{s}$, the maxima with respect to σ^2 is given by

$$\sigma^2{}_{opt} = \frac{1}{NL}\sum_{t=1}^{N}\left|\mathbf{x}(t)-\mathbf{A}(\boldsymbol{\theta})\mathbf{s}(t)\right|^2 \tag{2.48}$$

Substituting (2.48) into (2.47) and ignoring the constant terms, the likelihood estimator is obtained from following maximization problem

$$\begin{aligned}\hat{\boldsymbol{\theta}} &= \arg\left\{\max_{\boldsymbol{\theta},\mathbf{S}}\left(-\ln\left[\sum_{t=1}^{N}\left\|\mathbf{x}(t)-\mathbf{A}(\boldsymbol{\theta})\mathbf{s}(t)\right\|^2\right]\right)\right\} \\ &= \arg\left\{\min_{\boldsymbol{\theta},\mathbf{S}}\left[\sum_{t=1}^{N}\left\|\mathbf{x}(t)-\mathbf{A}(\boldsymbol{\theta})\mathbf{s}(t)\right\|^2\right]\right\}\end{aligned} \tag{2.49}$$

Fixing $\boldsymbol{\theta}$, the minima with respect to $\mathbf{s}(t)$ is given by

$$\mathbf{s}_{opt}(t) = \mathbf{A}^{+}(\boldsymbol{\theta})\mathbf{x}(t) \tag{2.50}$$

where

$$\mathbf{A}^{+}(\boldsymbol{\theta}) = \left(\mathbf{A}^{H}(\boldsymbol{\theta})\mathbf{A}(\boldsymbol{\theta})\right)^{-1}\mathbf{A}^{H}(\boldsymbol{\theta}) \tag{2.51}$$

is the pseudo-inverse of $\mathbf{A}(\boldsymbol{\theta})$.

Substituting (2.50) into (2.49), the ML estimator is given by

$$\hat{\boldsymbol{\theta}} = \arg\left\{\min_{\boldsymbol{\theta},\mathbf{S}}\left[\sum_{t=1}^{N}\left\|\mathbf{x}(t)-\mathbf{P}(\boldsymbol{\theta})\mathbf{s}(t)\right\|^2\right]\right\} \tag{2.52}$$

where $\mathbf{P}(\boldsymbol{\theta}) = \mathbf{A}(\boldsymbol{\theta})\left(\mathbf{A}^{H}(\boldsymbol{\theta})\mathbf{A}(\boldsymbol{\theta})\right)^{-1}\mathbf{A}^{H}(\boldsymbol{\theta})$. The DOAs can be found by using a mul-

tidimensional search.

The ML estimator also can be written in the form of [13]

$$\begin{aligned}\hat{\boldsymbol{\theta}} &= \arg\left\{\min_{\boldsymbol{\theta}} \mathrm{Tr}\left\{(\mathbf{I}-\boldsymbol{\Pi}_{\mathbf{A}})\hat{\mathbf{R}}\right\}\right\} \\ &= \arg\left\{\min_{\boldsymbol{\theta}} \frac{1}{N}\sum_{t=1}^{N}\left\|(\mathbf{I}-\boldsymbol{\Pi}_{\mathbf{A}})\hat{\mathbf{R}}\right\|^2\right\}\end{aligned} \tag{2.53}$$

where

$$\hat{\mathbf{R}} = \frac{1}{N}\sum_{t=1}^{N}\mathbf{x}(t)\mathbf{x}^H(t), \tag{2.54}$$

$$\boldsymbol{\Pi}_{\mathbf{A}} = \mathbf{A}(\boldsymbol{\theta})\mathbf{A}^{+}(\boldsymbol{\theta}). \tag{2.55}$$

This is because for any vector $\mathbf{x}$, $\|\mathbf{x}\|^2 = \mathrm{Tr}\{\mathbf{x}\mathbf{x}^H\}$. Here Tr denotes the trace of a matrix.

An interpretation for (2.53) is that the observed signals $\mathbf{x}(t)$ are projected to a model subspace orthogonal to all signal components, and the power of projected signal is measured. The ML estimator approaches to minimum power when the projector removes all the true signals ($\hat{\boldsymbol{\theta}} \to \boldsymbol{\theta}_0$). But when finite samples are used to estimate the signal covariance matrix $\hat{\mathbf{R}}$, the result of estimator will have a certain bias with respect to the true DOAs. The bias will converge to zero if the number of samples is increased to infinity [8].

To find the optimization results of (2.53), a non-linear *M*-dimension search has to be performed. Given a set of initial guess value of unknown parameters, some search methods such as steepest descent method, Gauss-Newton method can be applied to find the optimum values. But if the initial guess is not accurate enough, the

search procedure may converge to a local minimum instead of the desired global minimum. We can use spectral-based method to give a rough estimation and then use this rough estimation as the initial guess for ML estimator.

2.6 Summary

DOA estimation is an important problem in radar, sonar and other localization systems. Beamforming techniques estimate directions by maximizing the output power of an antenna array. These techniques are easy to implement, but they do not have a sufficiently high resolution and it is also difficult for them to distinguish closely spaced signal sources. Furthermore, the performance of beamforming techniques degrades quickly at low signal-to-noise ratio when compared with other methods.

Subspace methods provide better performance as they exploit the eigen-structure of the covariance matrix of received signals. Most subspace methods are consistent methods, implying that the estimations converge to the true values of parameters as the number of samples tends to infinity. The resolution of subspace methods is much higher than that of beamforming techniques. However, it is not easy for conventional subspace methods to estimate the directions of highly correlated signals, especially the coherent signals which would cause the rank of the covariance matrix of the received signal to be deficient. However, the forward and backward spatial averaging method based on subspace methods can be applied to distinguish coherent sources. The spatial smoothing method is to split the ULA into a number of over-

lapping sub-arrays and the steering vectors for sub-arrays are identical up to different scalings, and then take the average of the sub-array covariance matrices. The forward spatial smoothing method needs $2M$ array elements to solve M DOAs [12]. If forward and backward spatial smoothing methods are combined together, $\frac{3}{2}M$ elements are needed to solve M coherent DOAs [14].

Maximum likelihood (ML) method is a powerful tool to solve any type of estimation problem provided that the joint probability distribution of observed data is known. The ML method requires doing a non-linear multidimensional search to find the estimates. Steepest descent method, Gauss-Newton method and other search methods can be applied to do this search. Usually the initial guess is important to apply these search methods because they may converge to a local minimum, so spectral-based methods can be used to find a rough estimate as the initial guess for ML estimator.

Chapter 3

Frequency Hopping Correlation (FHC) Method to Track Multipath Signals for Frequency Hopping System

3.1 Introduction to the DOA estimation for frequency hopping system

In this chapter, we will discuss the problem of estimating and tracking the directions for multipath signals in frequency hopping systems. In the conventional DOA estimation methods, the steering vector may not change with respect to time, but in a frequency hopping system the steering vector changes with respect to time or hops as the frequency of transmitted signal varies with respect to time. Therefore the conventional methods may not solve the DOA for the frequency hopping system directly. For example, given an ULA as the receiving array, the received signal is

$$\mathbf{x}(t) = \mathbf{a}(\theta)s(t) \tag{3.1}$$

where

$$\mathbf{a}(\theta) = g(\theta)\begin{bmatrix} 1 & e^{-j\frac{2\pi f}{c}d\sin\theta} & \dots & e^{-j(L-1)\frac{2\pi f}{c}d\sin\theta} \end{bmatrix}^{\mathrm{T}}. \tag{3.2}$$

It is clear that the steering vector is dependent on the frequency.

Some techniques have been developed for the DOA estimation in frequency hopping systems. In [15], Wong proposed an eigen-value decomposition based method for wideband fast frequency hopping signals. This method needs an electromagnetic

sensor as the receiving array. This is because the steering vector of electromagnetic sensors is not dependent on frequency. Therefore the conventional method is applicable. However, the electromagnetic sensors are expensive and difficult to manufacture. In [16] Liu *et al* proposed a method based on signal spectral entropy to estimate the hop instant and the least square method is applied to estimate direction for hop-free data. This method jointly estimates frequency and direction based on hop detection but it does not consider the multipath. In [29] Fuchs proposed a method to estimate time delay and number of paths for multipath sources, but it is not applicable for the frequency hopping signals. For the well known maximum likelihood method [25] and the conventional least square method [26], the transmitted signal is required to be known. And all these methods need a large size antenna array at the receiver.

The proposed FHC method can estimate and track the directions of multipath signals in frequency hopping systems with a two-element array.

3.2 Signal Model for the FHC method

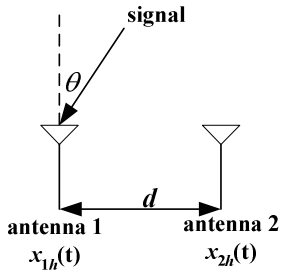

Fig. 3.1 Receiving array structure.

Let us consider a scenario where there is only one far-field transmitter and the receiving array is a two-element array with half wavelength spacing. The quadrature modulated transmitted signal is a hop sequence given by

$$d(t) = s(t)e^{j(\omega_c+\omega_h)t} \cdot u(t - hT_d) \tag{3.3}$$

where $f_h = \frac{\omega_h}{2\pi}$ is the hop frequency, $f_c = \frac{\omega_c}{2\pi}$ is the carrier frequency, $s(t)$ is the complex baseband signal, T_d is the hop duration, and *h* is the hop index.

For simplificity, the received signals can be considered hop by hop. So for a certain *h*th hop, the transmitted signal is

$$d_h(t) = s_h(t)e^{j(\omega_c+\omega_h)t}. \tag{3.4}$$

Here, we assume that there are some identical data packets for each hop. This assumption is reasonable as these packets may be the address headers or the synchronization bits. For example, the Bluetooth standard specifies that 72 bits are used as access code and 54 bits are used as header information in each packet [17], and the access code is used for synchronization and is the same for all packets. In SFH based PCS system, there are also specifications similar [18] to those of Bluetooth. Thus it is reasonable to assume that there are some identical data for each hop. This assumption also implies that the transmitted signal is a slow frequency hopping (SFH) signal, so it can be guaranteed that there is more than one bit in each hop. We also have another assumption that the hop instant and frequencies are known. Thus, (3.4) can be written as

$$d_h(t) = s(t)e^{j(\omega_c+\omega_h)t} \tag{3.5}$$

If the transmitted signal passes through p paths, the received signals at two antennas are

$$x_{1h}(t)=\sum_{p=0}^{P-1} g_p s(t) e^{j(\omega_c+\omega_h)(t-\tau_p)}+q_1(t) \tag{3.6}$$

$$x_{2h}(t)=\sum_{p=0}^{P-1} g_p s(t) e^{j(\omega_c+\omega_h)(t-\tau_p-\beta_p(h))}+q_2(t) \tag{3.7}$$

where $\beta_p(h)=\dfrac{d\sin\theta_p(h)}{c}$, c is the speed of light, $\theta_p(h)$ is the angle of arrival of the pth path and it changes with respect to time or hops, $g_p=\rho_p e^{j\phi_p}$ is the complex channel attenuation factor of the pth path, ρ_p and ϕ_p are amplitude and phase of g_p respectively, $q_1(t)$ and $q_2(t)$ are uncorrelated white Gaussian noise.

The received signal is down converted and passes a bandlimted filter. We have

$$x_{1h}(t)=\sum_{p=0}^{P-1} \rho_p e^{j\phi_p} s(t) e^{j\omega_h t} e^{-j(\omega_c+\omega_h)\tau_p}+q_1(t) \tag{3.8}$$

$$x_{2h}(t)=\sum_{p=0}^{P-1} \rho_p e^{j\phi_p} s(t) e^{j\omega_h t} e^{-j(\omega_c+\omega_h)(\tau_p+\beta_p(h))}+q_2(t) \tag{3.9}$$

It should be noted that the hopping frequency is not removed at the receiver, which is different from ordinary frequency hopping receivers. This is because some features of the hopping frequency will be exploited in the proposed method.

The power and cross correlation of received signals are given by

$$\mathrm{E}\left[\left|x_{1h}(t)\right|^2\right]=\left|\sum_{p=0}^{P-1} \rho_p e^{j\phi_p} e^{-j(\omega_c+\omega_h)\tau_p}\right|^2\cdot\mathrm{E}\left|s(t)\right|^2+P_{n1} \tag{3.10}$$

$$\mathrm{E}\left[\left|x_{1h}(t)\right|^2\right]=\left|\sum_{p=0}^{P-1} \rho_p e^{j\phi_p} e^{-j(\omega_c+\omega_h)(\tau_p+\beta_p(h))}\right|^2\cdot\mathrm{E}\left|s(t)\right|^2+P_{n2} \tag{3.11}$$

$$\mathrm{E}\left[x_{1h}{}^{*}(t)x_{2h}(t)\right]=\left[\sum_{p=0}^{P-1}\rho_p e^{j\phi_p}e^{-j(\omega_c+\omega_h)\tau_p}\right]^{*}\left[\sum_{p=0}^{P-1}\rho_p e^{j\phi_p}e^{-j(\omega_c+\omega_h)(\tau_p+\beta_p(h))}\right]\cdot\mathrm{E}\left|s(t)\right|^2 \tag{3.12}$$

where P_{n1} and P_{n2} are powers of $q_1(t)$ and $q_2(t)$, respectively.

3.3 Formulation of the FHC method

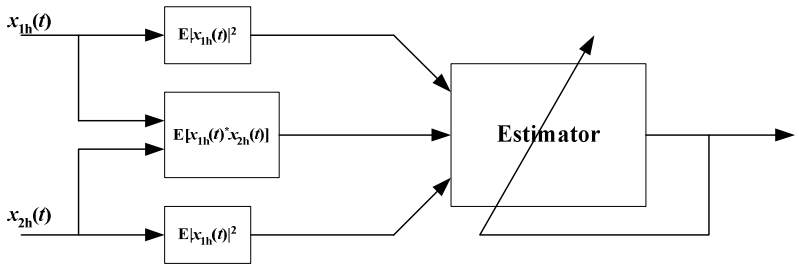

Fig. 3.2 System Structure for one hop

The objective function is formulated by minimizing the difference between the measured correlations of the received signals and their estimated values. In Fig. 3.2, the power and cross correlation of received signal can be measured by using analog correlators. Then an adaptive estimator is used to estimate the unknown parameters. By using least square method, the objection function is established as shown in (3.13).

$$f(\boldsymbol{\eta})=\sum_{h=k}^{k+N}\left\{\begin{array}{l}\left|\left[\sum_{p=0}^{P-1}\rho_p e^{j\phi_p}e^{-j(\omega_c+\omega_h)\tau_p}\right]^{*}\left[\sum_{p=0}^{P-1}\rho_p e^{j\phi_p}e^{-j(\omega_c+\omega_h)(\tau_p+\beta_p(h))}\right]\cdot\mathrm{E}\left|s(t)\right|^2+P_{n1}-r_{1h}\right|^2\\ +\left|\left[\sum_{p=0}^{P-1}\rho_p e^{j\phi_p}e^{-j(\omega_c+\omega_h)(\tau_p+\beta_p(h))}\right]^{*}\left[\sum_{p=0}^{P-1}\rho_p e^{j\phi_p}e^{-j(\omega_c+\omega_h)(\tau_p+\beta_p(h))}\right]\cdot\mathrm{E}\left|s(t)\right|^2+P_{n2}-r_{2h}\right|^2\\ +\left|\left[\sum_{p=0}^{P-1}\rho_p e^{j\phi_p}e^{-j(\omega_c+\omega_h)\tau_p}\right]^{*}\left[\sum_{p=0}^{P-1}\rho_p e^{j\phi_p}e^{-j(\omega_c+\omega_h)(\tau_p+\beta_p(h))}\right]\cdot\mathrm{E}\left|s(t)\right|^2-c_h\right|^2\end{array}\right\} \tag{3.13}$$

In (3.13) $\boldsymbol{\eta}=\left[\boldsymbol{\rho}\quad\boldsymbol{\theta}\quad\boldsymbol{\Delta\varphi}\quad\boldsymbol{\Delta\tau}\quad P_{n1}\quad P_{n2}\right]^{\mathrm{T}}$ is the parameter vector to estimate,

$\boldsymbol{\Delta\tau} = [\tau_1 - \tau_0 \quad \tau_2 - \tau_0 \quad ... \quad \tau_{P-1} - \tau_0]$ is the relative time delay vector, $\boldsymbol{\rho} = [\rho_0 \quad \rho_1 \quad ... \quad \rho_{p-1}]$, $\boldsymbol{\Delta\varphi} = [\phi_1 - \phi_0 \quad \phi_2 - \phi_0 \quad ... \quad \phi_{p-1} - \phi_0]$ are amplitude and phase vectors of channel attenuation factors respectively, $\boldsymbol{\theta} = [\theta_0 \quad \theta_1 \quad ... \quad \theta_{P-1}]$ is the DOA vector, P_{n1} and P_{n2} are the estimated powers of the white noise at two receiving antennas, r_{1h}, r_{2h} and c_h are measured signals' power and cross correlation, respectively of the *h*th hop, *k* is an integer and increased by one along hops, *N* is the number of hops used in one iteration. It is easy to see that the objective function is zero when the estimated parameters are at their true values for the stationary FH signals (stationary means the emitter does not move).

For each single hop, the objective function is periodic with respect to $\boldsymbol{\Delta\tau}$ and is not resolvable. The objective function can be written as

$$f(\boldsymbol{\eta}) = \sum_{h=k}^{k+N} \left[|L_{1h}(\boldsymbol{\eta})|^2 + |L_{2h}(\boldsymbol{\eta})|^2 + |L_{3h}(\boldsymbol{\eta})|^2 \right] \tag{3.14}$$

If only one hop frequency is used, the first term of (3.13) will be

$$L_1(\boldsymbol{\eta}) = \left| \sum_{p=0}^{P-1} \rho_p e^{j\phi_p} e^{-j(\omega_c + \omega_1)\tau_p} \right|^2 \cdot \mathrm{E}|s(t)|^2 + P_{n1} - r_{11} \tag{3.15}$$

We note that $L_1(\boldsymbol{\eta})$ is periodic with respect to the time delay vector $\boldsymbol{\Delta\tau}$ and the period is $T_1 = \dfrac{2\pi}{\omega_c + \omega_1}$. Thus the optimum value can not be found in the one hop case because many values other than the true value are also optimum values for the objective function. Fig. 3.3 shows a two-path case with carrier frequency at 30MHz. $\Delta\tau = \tau_1 - \tau_0$. The true value of $\Delta\tau$ is 0.5×10^{-5} seconds.

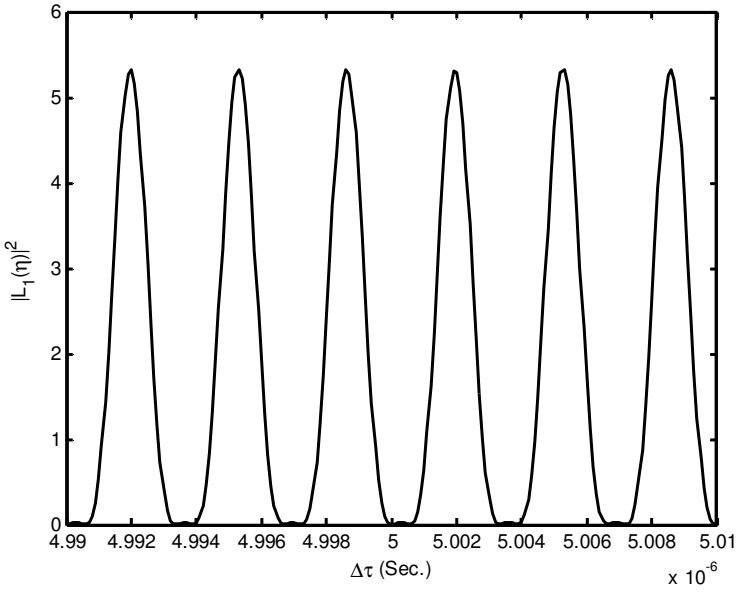

Fig. 3.3 The objective function w.r.t $\Delta\tau$ with one hop frequency

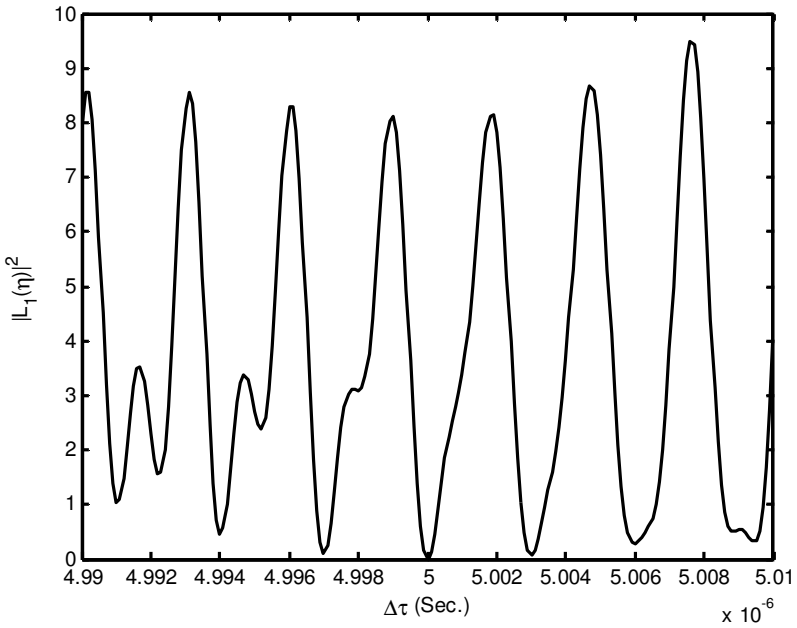

Fig. 3.4 The objective function w.r.t $\Delta\tau$ with two hop frequencies

However, for another hop with different hop frequency f_2, the period of $L_1(\boldsymbol{\eta})$

changes to $T_2 = \frac{2\pi}{\omega_c + \omega_2}$. If more hops are combined together, $\sum |L_1(\boldsymbol{\eta})|^2$ may not be periodic because the common multiples of these hop frequencies may not exist. Even when only two hop frequencies are used and they have a common multiple, the least common multiple may be very large if the hop frequencies are well selected. Then there will be no other optimum values around the true value. Fig. 3.4 shows a two-path case when two hops are combined together. Parameters are the same as the one hop case. Therefore we can use hops 1, 2,…, *N* in the first iteration, then use hops 2,3,…, *N*+1 in the next iteration and continue in this manner. The objective function is formulated as in (3.13). Usually *N* is chosen to be two or three.

3.4 Search Methods

3.4.1 Steepest Descent Method

The objective function is a non-linear least square function, and the optimum values can be found by using some search methods. Steepest Descent method, Newton method and Gauss-Newton method are all widely used in optimization problems. First, we will introduce Steepest Descent method, which is one of the fundamental procedures for minimizing a differentiable convex function of several variables. Because the gradient of a function or a surface is the vector that points to the maximum increase in the value of the function or the surface, it is obvious that moving along the opposite direction means going towards the minimum [19]. The

Steepest Descent method converges to a point with zero gradient. In Fig.3.5, the ellipses are the contours of $f(x_1, x_2)$. It shows that how the Steepest Descent method works. The formulation of Steepest Descent method is

$$\mathbf{x}(n+1) = \mathbf{x}(n) - \mu \nabla_{\mathbf{x}} f(\mathbf{x}) \tag{3.16}$$

where *n* is the iteration index, μ is a small number to control the step size.

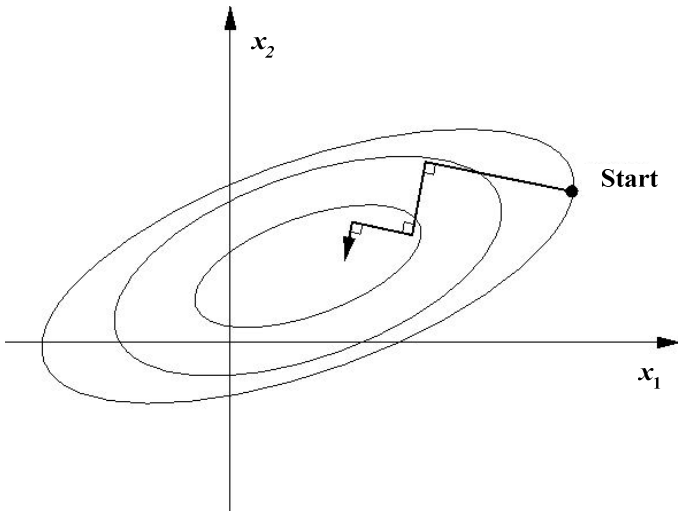

Fig. 3.5 Illustration of steepest descent method.

The method of Steepest Descent performs very well in early stages of the search process if the initial point is well selected (this means the initial point is on the convex surface around the optimum value). However, as a stationary point is approached, the method usually behaves poorly. This is because when the step size is relatively big, the iteration result will be oscillatory around the optimum point in the later stage of iterations. But if the step size is very small, the number of iterations from initial value to optimum point will be extremely large. Therefore the method of Steepest Descent is suitable for a problem where some *a prior* information of the minimum is known so that a good initial value and step size can be selected to solve the problem.

3.4.2 Newton's Method

The Newton's method is a procedure that deflects the steepest descent by premultiplying it by the inverse of the Hessian matrix.

$$\mathbf{x}(n+1) = \mathbf{x}(n) - \mathbf{H}^{-1}\nabla_{\mathbf{x}} f(\mathbf{x})\Big|_{\mathbf{x}=\mathbf{x}(n)} \tag{3.17}$$

where $\nabla_{\mathbf{x}} f(\mathbf{x}) = \left[\begin{array}{cccc} \frac{\partial f(\mathbf{x})}{\partial x_1} & \frac{\partial f(\mathbf{x})}{\partial x_2} & \cdots & \frac{\partial f(\mathbf{x})}{\partial x_n} \end{array}\right]^{\mathrm{T}}$, and

$\mathbf{H} = \begin{pmatrix} \frac{\partial^2 f(\mathbf{x})}{\partial x_1^2} & \frac{\partial^2 f(\mathbf{x})}{\partial x_1 \partial x_2} & \cdots & \frac{\partial^2 f(\mathbf{x})}{\partial x_1 \partial x_k} \\ \frac{\partial^2 f(\mathbf{x})}{\partial x_2 \partial x_1} & \frac{\partial^2 f(\mathbf{x})}{\partial x_2^2} & \cdots & \frac{\partial^2 f(\mathbf{x})}{\partial x_2 \partial x_k} \\ \cdots & \cdots & \cdots & \cdots \\ \frac{\partial^2 f(\mathbf{x})}{\partial x_k \partial x_1} & \frac{\partial^2 f(\mathbf{x})}{\partial x_k \partial x_2} & \cdots & \frac{\partial^2 f(\mathbf{x})}{\partial x_k^2} \end{pmatrix}$ is the Hessian matrix of $f(\mathbf{x})$.

The Newton's method is applicable to the same scenario of the steepest descent method and it has a quadratic convergence for quadratic surfaces, which is much faster than the steepest descent method. The Newton's method is derived from the second order Taylor expansion

$$f(\mathbf{x}) \approx f[\mathbf{x}(n)] + \nabla_{\mathbf{x}} f[\mathbf{x}(n)]^{\mathrm{T}} \cdot [\mathbf{x} - \mathbf{x}(n)] + \frac{1}{2}[\mathbf{x} - \mathbf{x}(n)]^{\mathrm{T}} \cdot \mathbf{H}[\mathbf{x}(n)] \cdot [\mathbf{x} - \mathbf{x}(n)] \tag{3.18}$$

In the Newton's method, the value of $\mathbf{x}$ of the next iterate is obtained from the minimizer of $f(\mathbf{x} + \Delta\mathbf{x})$. If the Hessian matrix is positive definite [20], the function $f(\mathbf{x})$ will have a unique minimum that can be obtained by solving

$$\nabla_{\mathbf{x}} f(\mathbf{x}) = \nabla_{\mathbf{x}} f[\mathbf{x}(n)] + \mathbf{H}[\mathbf{x}(n)] \cdot [\mathbf{x} - \mathbf{x}(n)] = 0 \tag{3.19}$$

Then we have

$$\Delta\mathbf{x} = -\mathbf{H}^{-1}\nabla f[\mathbf{x}(n)] = -\mathbf{H}^{-1}\nabla f(\mathbf{x})\Big|_{\mathbf{x}=\mathbf{x}(n)} \tag{3.20}$$

Although the Newton's method has a better convergence behavior than steepest descent does, it also has some drawbacks. One is the computation for the Hessian matrix is very complex if the size of parameter vector $(x_1,...,x_n)$ is too large. The calculation of the inversion of the Hessian matrix has to do n^3 multiplications. Another drawback is that the Hessian matrix may be singular during the iteration, or the searching direction $-\mathbf{H}^{-1}\nabla f(\mathbf{x})\big|_{\mathbf{x}=\mathbf{x}(n)}$ may not be a descent direction. To improve the Newton's method, many techniques are developed based on Newton's method.

3.4.3 Gauss-Newton Method

The Gauss-Newton method is suitable for small-residual non-linear least square problems. It is based on the Newton's method. The meaning of small-residue will be explained later.

Usually the least square method is used in data-fitting problems. Suppose a physical process is modeled by a nonlinear function ϕ that depends on parameter vector $\mathbf{x}$ and time *t*. If b_i is the actual output of the system at time t_i, then the residue is $L_i(\mathbf{x}) = \phi(\mathbf{x}, t_i) - b_i$, which is the difference between the predicted value ϕ and observed output b_i. When the residue is small or closed to zero, the problem is called small-residue nonlinear least square problem. A least square equation is formulated based on this difference

$$f(\mathbf{x}) = \frac{1}{2}\|\mathbf{l}(\mathbf{x})\|_2^{\,2} \tag{3.21}$$

where $\mathbf{l}(\mathbf{x}) = [l_1(\mathbf{x}) \quad ... \quad l_n(\mathbf{x})]^{\mathrm{T}}$.

The first order derivative of $f(\mathbf{x})$ with respect to x_i is

$$\nabla_{\mathbf{x}} f(\mathbf{x}) = \nabla_{\mathbf{x}} \mathbf{l}(\mathbf{x})^{\mathrm{T}} \cdot \mathbf{l}(\mathbf{x}) \tag{3.22}$$

where $\nabla_{\mathbf{x}} f(\mathbf{x}) = [\nabla_{x_1} f(\mathbf{x}),...,\nabla_{x_i} f(\mathbf{x})]^{\mathrm{T}}$, $\nabla_{\mathbf{x}} \mathbf{l}(\mathbf{x}) = [\nabla_{x_1} \mathbf{l}(\mathbf{x}) \quad ... \quad \nabla_{x_n} \mathbf{l}(\mathbf{x})]^{\mathrm{T}}$, $\nabla_{x_k} \mathbf{l}(\mathbf{x}) = [\nabla_{x_1} l_1(\mathbf{x}) \quad ... \quad \nabla_{x_n} l_n(\mathbf{x})]^{\mathrm{T}}$.

The Hessian matrix is also the second order derivative of $f(\mathbf{x})$, and it is given by

$$\nabla_{\mathbf{x}}^{\,2} f(\mathbf{x}) = \nabla_{\mathbf{x}} \mathbf{l}(\mathbf{x})^{\mathrm{T}} \cdot \nabla_{\mathbf{x}} \mathbf{l}(\mathbf{x}) + \sum_{i=1}^{n} l_i(\mathbf{x}) \nabla_{\mathbf{x}}^{\,2} l_i(\mathbf{x}) \tag{3.23}$$

In many practical circumstances, the first term $\nabla_{\mathbf{x}} \mathbf{l}(\mathbf{x})^{\mathrm{T}} \cdot \nabla_{\mathbf{x}} \mathbf{l}(\mathbf{x})$ of the Hessian matrix is more important than the second term, especially when the residuals $l_i(\mathbf{x})$ are small enough at the optimum values. To be more specifically, the small-residual problem is defined such that for all **x** closed to the optimum solution, the quantities $l_i(\mathbf{x}) \nabla_{\mathbf{x}}^{\,2} l_i(\mathbf{x})$ are small compared to the smallest eigenvalue of $\nabla_{\mathbf{x}} \mathbf{l}(\mathbf{x})^{\mathrm{T}} \cdot \nabla_{\mathbf{x}} \mathbf{l}(\mathbf{x})$.

The Gauss-Newton method is developed to solve the small-residual least square problem. In Gauss-Newton method, the second term of the Hessian matrix is ignored in (3.23) for its value is relatively small. Then we only substitute the first term of (3.23) and (3.22) into the formulation of Newton's method and we get

$$\mathbf{x}(n+1) = \mathbf{x}(n) - l'(\mathbf{x}_n)^{+} l(\mathbf{x}_n) \tag{3.24}$$

where

$$l'(\mathbf{x}_n)^{+} = [\nabla_{\mathbf{x}} l(\mathbf{x}_n)^{\mathrm{T}} \cdot \nabla_{\mathbf{x}} l(\mathbf{x}_n)]^{-1} \cdot \nabla_{\mathbf{x}} l(\mathbf{x}_n)^{\mathbf{T}} \tag{3.25}$$

is the Moore-Penrose pseudo-inverse of the matrix $\nabla_{\mathbf{x}} l(\mathbf{x}_n)$.

We can see that $l(\mathbf{x}_n)$ is closed to zero when $\mathbf{x}_n$ is around its optimum value. Thus $\nabla_{\mathbf{x}} l(\mathbf{x}_n)^{\mathrm{T}} \cdot \nabla_{\mathbf{x}} l(\mathbf{x}_n)$ will be singular and it is impossible to calculate its inversion and the Gauss-Newton method is not applicable. A method to solve this problem is to add an identity matrix $\mathbf{S}_n$ multiplied by a scalar with small values. in the Gauss-Newton iteration equation

$$\mathbf{x}(n+1) = \mathbf{x}(n) - \left[\nabla_{\mathbf{x}} l(\mathbf{x}_n)^{\mathrm{T}} \cdot \nabla_{\mathbf{x}} l(\mathbf{x}_n) + \mathbf{S}_n\right]^{-1} \cdot \nabla_{\mathbf{x}} l(\mathbf{x}_n)^{\mathrm{T}} \cdot l(\mathbf{x}_n) \tag{3.26}$$

The purpose of $\mathbf{S}_n$ is to guarantee fast convergence and avoid the matrix singularity in the matrix inversion.

To apply the Gauss-Newton method in our problem, it should be made sure that our problem meets the required conditions of Gauss-Newton method. The objective function (3.13) can be written as

$$f(\boldsymbol{\eta}) = \sum_h \sum_i \left| L_{i,h}(\boldsymbol{\eta}) \right|^2 \tag{3.27}$$

where $L_i(\boldsymbol{\eta})$ is the *i*th summation term of (3.13) respectively.

We can see that $L_{i,h}(\boldsymbol{\eta})$ are all closed to zero if $\boldsymbol{\eta}$ is around its optimum value. This means our problem is a small-residual problem. Thus Gauss-Newton method can be applied to it. If we define $L(\boldsymbol{\eta}) = [L_1(\boldsymbol{\eta}) \quad L_2(\boldsymbol{\eta}) \quad L_3(\boldsymbol{\eta})]^{\mathrm{T}}$, the Jacobian matrix of $L(\boldsymbol{\eta})$ is

$$J(\boldsymbol{\eta}) = \left(\frac{\partial L(\boldsymbol{\eta})}{\partial \boldsymbol{\eta}(1)} \quad \cdots \quad \frac{\partial L(\boldsymbol{\eta})}{\partial \boldsymbol{\eta}(n)} \right)^{\mathrm{T}} \tag{3.28}$$

The parameter vector $\boldsymbol{\eta}$ is updated in the following manner

$$\boldsymbol{\eta}_{k+1} = \boldsymbol{\eta}_k - J(\boldsymbol{\eta}_k)^+ L(\boldsymbol{\eta}_k) \tag{3.29}$$

where $J(\boldsymbol{\eta}_k)^+ = \left(J(\boldsymbol{\eta}_k)^T J(\boldsymbol{\eta}_k) + \xi\right)^{-1} J(\boldsymbol{\eta}_k)^T$, ξ is an identity matrix multiplied by a scalar with small values.

Given an appropriate initial value of $\boldsymbol{\eta}$, the converged result will be the optimum value of $\boldsymbol{\eta}$.

3.4.4 Alternating Minimization Method

In many cases, a multi-dimensional search is needed to find the optimized values. Sometimes there may be a variable whose gradient is quite close to zero that the objective function is very flat with respect to this variable. If joint search methods (steepest descent method, Newton's method, etc) are used in this case, the parameters may converge very slowly. The alternating minimization method is suitable to solve this problem. Let us see how the alternating minimization method works.

Suppose we have an objective function given by

$$\boldsymbol{\eta} = \arg\min_{\boldsymbol{\eta}} f(\boldsymbol{\eta}) \tag{3.30}$$

where $\boldsymbol{\eta} = [\eta_1 \quad \eta_2 \quad \ldots \quad \eta_n]^T$. Given an initial value of $\boldsymbol{\eta}$, the first iteration is done with respect to η_1 until it is converged while other parameters are held fixed, then the second iteration is done to η_2 until it is converged with other parameter fixed and continue in this manner. That is, the value of η_i at the (k+1)th iteration is obtained by solving the following one-dimensional minimization problem:

$$\eta_i^{(k+1)} = \arg\min_{\eta_i} f\left(\boldsymbol{\eta}_i^{(k)}, \eta_i\right) \tag{3.31}$$

where $\boldsymbol{\eta}_i^{(k)}$ denotes the $(n-1)\times 1$ vector of pre-computed parameters,

$$\boldsymbol{\eta}_i^{(k)} = \left[\eta_1^{(k)}, \ldots \eta_{i-1}^{(k)}, \eta_{i+1}^{(k)}, \ldots \eta_n^{(k)}\right] \tag{3.32}$$

The difference between alternating minimization method and direct minimization method (steepest descent method, Newton's method, etc) is that the alternating minimization method progresses towards the bottom of $f(\boldsymbol{\eta})$ along parallel line to the axes [21], as Fig. 3.6 shows a two-dimensional case. We can see that the two parameter declines to the minimum alternately but in the traditional steepest descent method the parameters directly declines to the minimum. We also can group the parameters into several groups and do similar routines as mentioned above.

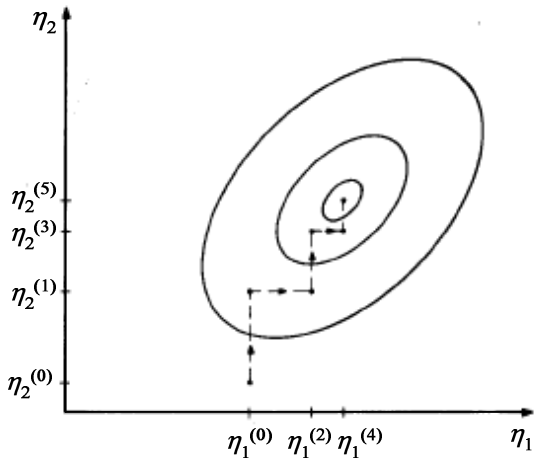

Fig. 3.6 Two-dimensional case of Alternating Minimization method.

3.5 Highly Oscillation problem

All search methods we introduced above require that the objective function is

convex or the initial guess is close enough to the optimum value. However, our objective function (3.13) is not convex but highly oscillatory with respect to the relative time delay $\boldsymbol{\Delta\tau}$. However, it is difficult to apply the search methods directly because the converged value may be a local minimum instead of the global minimum. We can see this problem in Fig. 3.7. Fig. 3.7 is plotted for a two-path case with the carrier frequency at 30MHz. Two hop frequencies are used in the objective function. It is clear the objective function is highly oscillatory and it is difficult to choose a suitable initial value for parameter vector $\boldsymbol{\eta}$.

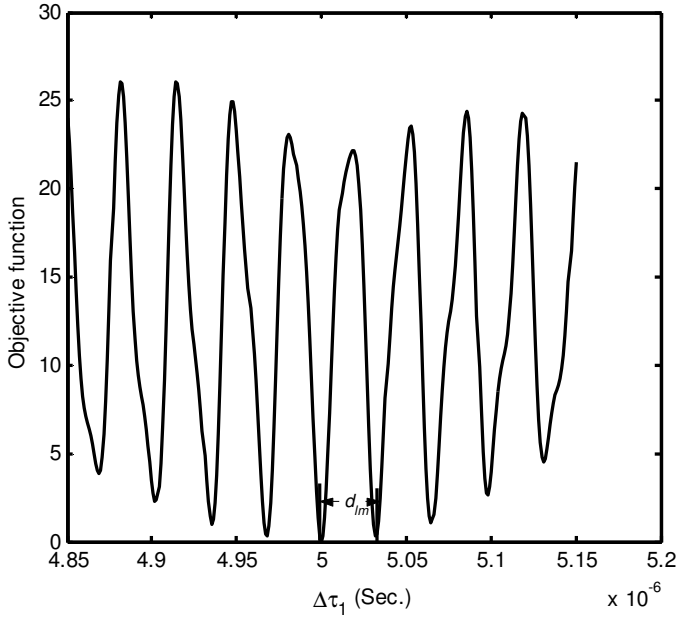

Fig. 3.7 The highly oscillatory objective function w.r.t time delay.

Although the objective function is highly oscillatory with respect to relative time delay, the distance between two adjacent local minima can be approximated. Here we still consider a two path case and $\boldsymbol{\Delta\tau} = \Delta\tau_1 = \tau_1 - \tau_0$. Suppose only two hop frequencies are used, ω_1 and ω_2, and the first term of (3.13) is

$$f_1(\boldsymbol{\eta}) = \sum_{h=1}^{2} \left| \left| \sum_{p=0}^{1} \rho_p e^{j\phi_p} e^{-j(\omega_c+\omega_h)\tau_p} \right|^2 \cdot \mathrm{E}|s(t)|^2 + P_{n1} - r_{1h} \right|^2$$
$$= \sum_{h=1}^{2} \left| \left| \rho_0{}^2 + \rho_1{}^2 + 2\rho_0\rho_1 \cos[\Delta\phi - (\omega_c+\omega_h)\Delta\tau] \right|^2 \cdot \mathrm{E}|s(t)|^2 + P_{n1} - r_{1h} \right|^2 \tag{3.33}$$

The power measurement r_{1h} is

$$r_{1h} = \left| \rho_{0\mathrm{T}}{}^2 + \rho_{1\mathrm{T}}{}^2 + 2\rho_{0\mathrm{T}}\rho_{1\mathrm{T}} \cos[\Delta\phi_{\mathrm{T}} - \alpha_h \Delta\tau_{\mathrm{T}}] \right|^2 \cdot \mathrm{E}|s(t)|^2 + P_{n1\mathrm{T}} \tag{3.34}$$

where $\alpha_h = \omega_c + \omega_h$, subscript T denotes the optimum value of corresponding parameter.

Without loss of generality we assume $\mathrm{E}|s(t)|^2 = 1$, which means the power of transmitted signal is a constant. Then, substituting (3.34) into (3.33), we have

$$f_1(\boldsymbol{\eta}) = \sum_{h=1}^{2} \left| \begin{array}{l} \rho_0{}^2 + \rho_1{}^2 - \rho_{0\mathrm{T}}{}^2 - \rho_{1\mathrm{T}}{}^2 + 2\rho_0\rho_1 \cos[\Delta\phi - \alpha_h\Delta\tau] \\ -2\rho_{0\mathrm{T}}\rho_{1\mathrm{T}} \cos[\Delta\phi_{\mathrm{T}} - \alpha_h\Delta\tau_{\mathrm{T}}] \end{array} \right|^2 + P_{n1} - P_{n1\mathrm{T}} \Bigg|^2$$
$$= \left\{ \begin{array}{l} (m - n\cos(\alpha_1\Delta\tau_{\mathrm{T}}) + 2\rho_0\rho_1\cos(\alpha_1\Delta\tau))^2 + \\ (m - n\cos(\alpha_2\Delta\tau_{\mathrm{T}}) + 2\rho_0\rho_1\cos(\alpha_2\Delta\tau))^2 \end{array} \right\} \tag{3.35}$$

where *m*, *n* are constants.

Taking differentiation to (3.33) with respect to relative time delay $\Delta\tau$, we have

$$\nabla_{\Delta\tau} f_1(\boldsymbol{\eta}) = \sum_{h=1}^{2} -4(m - n\cos(\alpha_h\Delta\tau_{\mathrm{T}}) + 2\rho_0\rho_1\cos(\alpha_h\Delta\tau))\rho_0\rho_1 a_h \sin(\alpha_h\Delta\tau) \tag{3.36}$$

To find the local extrema (minima and maxima) of $f(\boldsymbol{\eta})$, the first order derivative should be zero. Since the difference between α_1 and α_2 is small, we assume $\alpha_1 \approx \alpha_2$ and we also assume $\cos(\alpha_1\Delta\tau_{\mathrm{T}}) \approx \cos(\alpha_2\Delta\tau_{\mathrm{T}})$. After trigonometric function transformation, (3.36) becomes

$$\sin\left(\frac{\alpha_1+\alpha_2}{2}\Delta\tau\right)\left[(m-n)\cos\left(\frac{\alpha_1-\alpha_2}{2}\Delta\tau\right)+\cos\left(\frac{\alpha_1+\alpha_2}{2}\Delta\tau\right)\cos(\alpha_1-\alpha_2)\Delta\tau\right]=0 \quad (3.37)$$

From (3.37) it is obvious that $\nabla_{\Delta\tau} f(\boldsymbol{\eta})=0$ when $\sin\left(\frac{\alpha_1+\alpha_2}{2}\Delta\tau\right)=0$. Thus the approximated distance between two adjacent local extrema of $f(\boldsymbol{\eta})$ is $\frac{1}{2f_c+f_1+f_2}$. Then the distance between two contiguous local minima is

$$d_{lm}=\frac{2}{(f_c+f_1)+(f_c+f_2)}. \quad (3.38)$$

Similarly we can show that the other two terms of the objective function (3.13) have the same property. Expand the three terms of Eq. (3.13). We can see $\Delta\tau$ appears only at the index of $e^{-j(\omega_c+\omega_h)\Delta\tau}$. It is easy to validate that the period of each single term of the objective function with respect to $\Delta\tau$ is $\frac{1}{f_c+f_1}$ when only one frequency f_1 is used. This is because $e^{-j(\omega_c+\omega_1)\Delta\tau}=e^{-j(\omega_c+\omega_1)\left(\Delta\tau+\frac{1}{f_c+f_1}\right)}$. Then when only frequency f_2 is used, the period will be $\frac{1}{f_c+f_2}$. So if f_1 and f_2 are used together, the distance between two adjacent local minima of the objective function should be a value between $\frac{1}{f_c+f_1}$ and $\frac{1}{f_c+f_2}$. Since we are trying to obtain a rough value of the period with respect to $\Delta\tau$, it is reasonable to use $\frac{2}{(f_c+f_1)+(f_c+f_2)}$ as the estimates of the time delay $\Delta\tau$.

Furthermore, if more than two hop frequencies are combined to formulate the objective function, we can find this distance as well and it is generally

$$d_{lm} = \frac{n}{(f_c + f_1) + \ldots + (f_c + f_n)}. \tag{3.39}$$

Therefore, the distance between two local minima is inverse proportional to the average frequency of all hop frequencies.

3.6 Detailed Algorithm of the FHC method

Recall the objective function (3.13)

$$f(\boldsymbol{\eta}) = \sum_{h=k}^{k+N} \left\{ \begin{array}{l} \left| \sum_{p=0}^{P-1} \rho_p e^{j\phi_p} e^{-j(\omega_c+\omega_h)\tau_p} \right|^2 \cdot \mathrm{E}|s(t)|^2 + P_{n1} - r_{1h} \Big|^2 \\ + \left| \sum_{p=0}^{P-1} \rho_p e^{j\phi_p} e^{-j(\omega_c+\omega_h)(\tau_p+\beta_p(t))} \right|^2 \cdot \mathrm{E}|s(t)|^2 + P_{n2} - r_{2h} \Big|^2 \\ + \left| \left[\sum_{p=0}^{P-1} \rho_p e^{j\phi_p} e^{-j(\omega_c+\omega_h)\tau_p} \right]^* \left[\sum_{p=0}^{P-1} \rho_p e^{j\phi_p} e^{-j(\omega_c+\omega_h)(\tau_p+\beta_p(t))} \right] \cdot \mathrm{E}|s(t)|^2 - c_h \right|^2 \end{array} \right\} \tag{3.40}$$

To find the optimum values of unknown parameters, a multi-dimensional search is needed. The objective function is also highly oscillatory with respect to relative time delay. We will use a method which combines alternating minimization method, steepest descent method and Gauss-Newton method to solve this problem. Let us consider a two-path case, the parameter vector is $\boldsymbol{\eta} = [\rho_0 \quad \rho_1 \quad \theta_0 \quad \theta_1 \quad \Delta\tau \quad \Delta\phi \quad P_{n1} \quad P_{n2}]$. The parameters can be grouped into two groups: one is $\Delta\tau$, the other is $[\rho_0 \quad \rho_1 \quad \theta_0 \quad \theta_1 \quad \Delta\phi \quad P_{n1} \quad P_{n2}]$, then alternating minimization can be applied. If the initial value of $\Delta\tau$ is well selected, usu-

ally Gauss-Newton method combined with alternating minimization method can find the optimized $\boldsymbol{\eta}$ in several hundreds iterations (or hops). However, because the objective function is highly oscillatory, it is difficult to obtain a good initial value of $\Delta\tau$ so that the search method may converge to local minimum easily. Therefore we have to use other method to solve this problem. An intuitive solution is to exploit the quasi-periodic feature of the objective function w.r.t $\Delta\tau$. When steepest descent method is applied to find a local minimum w.r.t. $\Delta\tau$, we may find other adjacent local minima w.r.t $\Delta\tau$ with following steps.

1) Given an initial value of $\Delta\tau$, use steepest descent method to get a converged value $\Delta\tau^{(1)}$.
2) Approximate the adjacent local minima by exploiting the feature that the distance between two local minima is about $d_{lm} = \dfrac{n}{(f_c + f_1) + \ldots + (f_c + f_n)}$ if n hop frequencies are used in the objective function.

   $$\Delta\tau^{(k)} = \Delta\hat{\tau}^{(k-1)} \pm 1/\left[f_c + (f_1 + \ldots + f_n)/n\right] \tag{3.42}$$

   In order to avoid the heavy computation, the search for local minima (include the global minimum) is limited in a range that $a \le \Delta\tau_1^{(k)} \le b$. This range [$a$,$b$] should guarantee that it contains the global minimum.

3) Use the first order Taylor expansion of $\nabla_{\Delta\tau} f(\boldsymbol{\eta})$ to find a more precise local minimum around $\Delta\tau^{(k)}$. That is

   $$\nabla_{\Delta\tau} f \approx a_0 + a_1\left(\Delta\tau - \Delta\tau^{(k)}\right) \tag{3.43}$$

   where $a_0 = \nabla_{\Delta\tau} f\Big|_{\Delta\tau=\Delta\tau^{(k)}}$, $a_1 = \nabla^2_{\Delta\tau} f\Big|_{\Delta\tau=\Delta\tau^{(k)}}$.

Let (3.43) be zero, a more precise local minimum around $\Delta\tau^{(k)}$ is approximated [22], and we will have

$$\Delta\hat{\tau}^{(k)} = -a_0 / a_1 + \Delta\tau^{(k)} \tag{3.44}$$

4) Go back to step 2) until $\Delta\hat{\tau}^{(k)}$ or $\Delta\tau^{(k)}$ exceed the range [*a*,*b*].

With above procedures we will obtain all local minima in the range [*a*,*b*]. We can substitute these local minima into the objective function and choose the one which minimizes the objective function as the refined initial value of $\Delta\tau$. This refined initial value of $\Delta\tau$ is enough close to the true value of the time delay so that the Gauss-Newton method can be directly applied. The above procedure is to estimate adjacent local minimum after one local minimum is found, to refine the result of step 2) by using Taylor expansion, and to estimate other local minima one by one.

To apply the Gauss-Newton method, we adjust the objective function a little by taking the square of the original objective function (3.13). The new objective function is $F(\boldsymbol{\eta}) = |f(\boldsymbol{\eta})|^2$. Using the refined initial values and applying the Gauss-Newton method with modified objective function, we have

$$\boldsymbol{\eta}(k+1) = \boldsymbol{\eta}(k) - \mathbf{f}'(\boldsymbol{\eta}(k))^{+} f(\boldsymbol{\eta}(k)) \tag{3.45}$$

where $\mathbf{f}'(\boldsymbol{\eta}(k))^{+} = \left[\mathbf{f}'(\boldsymbol{\eta}(k))^{H}\mathbf{f}'(\boldsymbol{\eta}(k)) + \mathbf{S}_n\right]^{-1}\mathbf{f}'(\boldsymbol{\eta}(k))^{H}$, and the first order derivative vector is given by

$$\mathbf{f}'(\boldsymbol{\eta}(k)) = \left[\frac{\partial f(\boldsymbol{\eta}(k))}{\partial \boldsymbol{\eta}_1}, \ldots, \frac{\partial f(\boldsymbol{\eta}(k))}{\partial \boldsymbol{\eta}_n}\right]. \tag{3.46}$$

Simulation for the proposed algorithm will be shown in next chapter.

3.7 Summary

In this chapter, the FHC method is proposed to track and estimate the direction of multipath signals for frequency hopping systems. The least square method is used to establish the objective function by minimizing the difference between estimated correlations and measured correlations. Since the objective function is highly oscillatory with respect to the time delay parameters, a pre-processing is used to find refined initial values for the time delay. The Gauss-Newton method is applied to search the optimum values for unknown parameters. We choose the Gauss-Newton method because the steepest descent method has a zigzag problem and the Newton's method requires the Hessian matrix of unknown parameters is positive definite. The simulation study for the proposed method and comparison with other techniques will be discussed in the next chapter.

Chapter 4

Simulation Study of the FHC method

In this chapter, simulation results will be presented to illustrate the performance of the FHC method. The proposed method is compared with the frequency hopping maximum likelihood method (FHML method) [23]. First we will describe the simulation scenario.

4.1 Simulation Scenario

In the simulation, we consider a frequency hopping system with a center frequency at $f_c = 30\text{MHz}$. The signal is transmitted from one far field source. The receiving array is a two-element array with half wavelength spacing of *d*=5m. The 32 hopping frequency channels occupy 8MHz bandwidth and have 0.25MHz channel spacing from 26MHz to 34MHz. The minimum frequency separation between adjacent hops is 0.75MHz by referring the IEEE Standard 802.11. Then a hop sequence with 32 hop frequencies is formed and it is transmitted repeatedly. Table 4.1 is an example of the hop sequence.

The transmitted baseband signal $s(t)$ in the objective function (3.13) is assumed to be one, which implies that the transmitted signal is same for all hops so that the

power $E|s(t)|^2$ of sampled signal are same for all hops. With this assumption, the transmitted signal is $s_h(t) = e^{j(\omega_c+\omega_h)t}$. In the simulation, only this part is generated for convenience.

	Ch.1-6	Ch.7-12	Ch.13-18	Ch.19-24	Ch.25-30	Ch.31-32
Frequencies (MHz)	26.25	32.25	30.5	28.75	27.0	33.0
	27.25	33.25	31.5	29.75	28.0	34.0
	28.25	26.5	32.5	30.75	29.0	
	29.25	27.5	33.5	31.75	30.0	
	30.25	28.5	26.75	32.75	31.0	
	31.25	29.5	27.75	33.75	32.0	

Tab. 4.1 An example of hop sequence

The number of paths is assumed to be two, and the time delay for two paths are $\tau_0 = 5\mu s$ and $\tau_1 = 10\mu s$ respectively. The channel attenuation factors are $g_0 = 0.75e^{j0.5}$ and $g_1 = 0.85e^{j1}$. Therefore the amplitude and phase difference between g_0 and g_1 are $\rho_0 = 0.75$, $\rho_1 = 0.85$ and $\Delta\phi = 0.5$ respectively. The directions of two paths are $\theta_0 = 30^\circ$ and $\theta_1 = 50^\circ$ for the stationary case, and we will discuss the moving case later. The signal to noise ratio (SNR) is defined as

$$\text{SNR} = 10\log_{10}(P_s / P_n) \tag{4.1}$$

where P_s is the average power of the received signal of the whole hop sequence while P_n is the noise power. For each hop, 256 samples are taken with a sampling frequency $f_s = 8\text{MHz}$ to measure the power and cross correlation of the received signal. So the time duration for each hop is 32μs. In practice, analog correlators can be used to measure the correlations of received signals.

The waveform of the received signal (real part) at two antennas is shown in Fig. 4.1. It is plotted when SNR=20db. The power and cross correlation of the received signals are plotted hop by hop in Fig. 4.2 and Fig. 4.3.

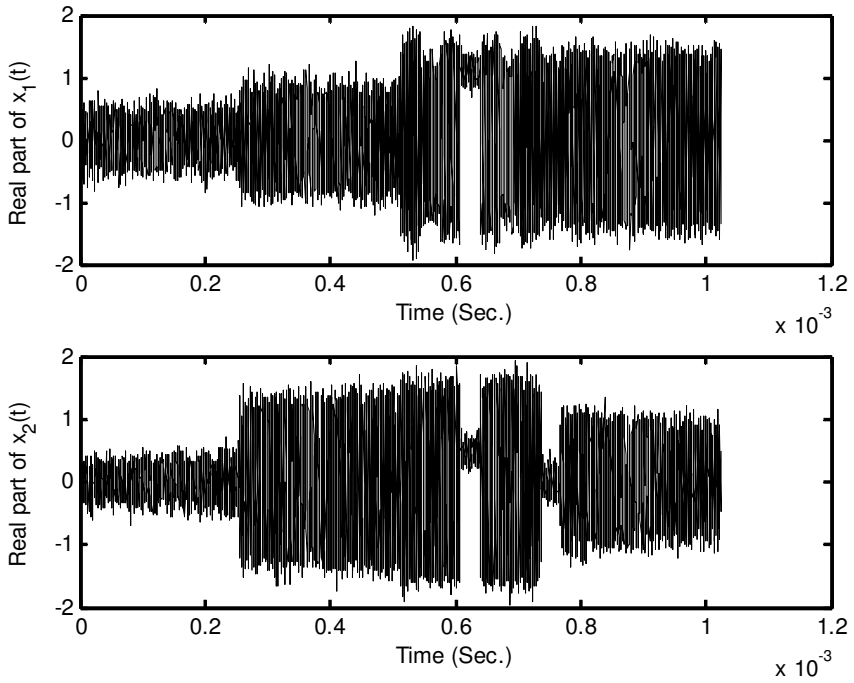

Fig. 4.1 Waveform of the received signals with AWGN.

It can be seen from Fig. 4.2 that the noise power contributes a lot in the power of the received signals. In Fig. 4.3, the cross correlation of received signals of two antennas is plotted in real part and imaginary part respectively. Theoretically, the cross correlation of noise free signals should be same as that of the signal with additive white noise. However, we can see small difference between the cross correlation of noise-free signals and that of signals with white noise in Fig. 4.3. This is because the samples of received signals are limited.

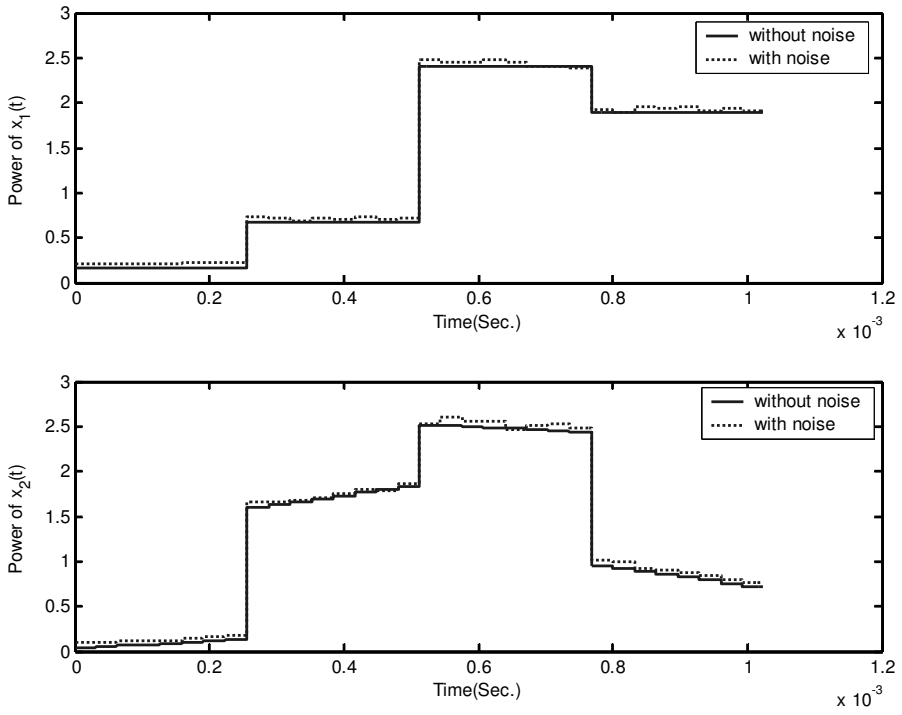

Fig. 4.2 Power of the received signals with AWGN and without AWGN

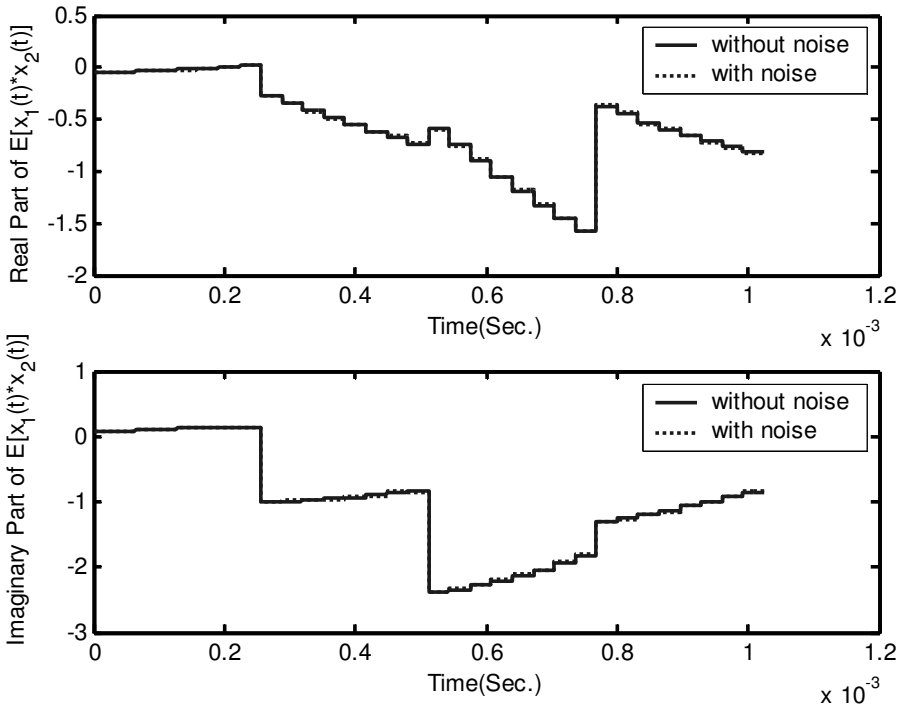

Fig. 4.3 Cross correlation of the received signals

4.2 Simulation of Estimating the Directions of Stationary FH signals

The initial parameter vector is set as follows

$$\hat{\boldsymbol{\eta}}(0) = \begin{bmatrix} 0.78 & 0.88 & 27^\circ & 47^\circ & 0.54 & 0.52\times 10^{-5} & 0.01405 & 0.0140 \end{bmatrix}^T$$

At the first step, a refined initial value of $\Delta\tau$ is calculated by applying (3.42), (3.43) and (3.44). Then the Gauss-Newton method is applied directly as follows

$$\boldsymbol{\eta}(k+1) = \boldsymbol{\eta}(k) - \mu \cdot \mathbf{f}'(\boldsymbol{\eta}(k))^{+} \mathbf{f}(\boldsymbol{\eta}(k)) \tag{4.2}$$

where

$$\mathbf{f}'(\boldsymbol{\eta}(k))^{+} = \left[\mathbf{f}'(\boldsymbol{\eta}(k))^{H} \mathbf{f}'(\boldsymbol{\eta}(k)) + \mathbf{S}_n\right]^{-1} \mathbf{f}'(\boldsymbol{\eta}(k))^{H} . \tag{4.3}$$

The small scaled identity matrix $\mathbf{S}_n$ is set to be $diag\left(10^{-7},...,10^{-7}\right)$. The step size is $\mu = 0.3$. Two successive hops are used to generate one result.

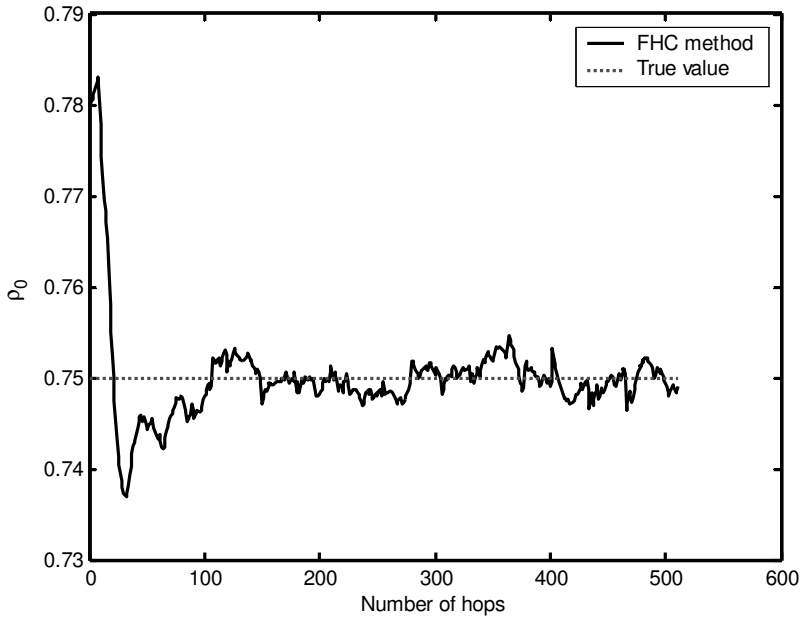

(a) ρ_0 vs. number of hops

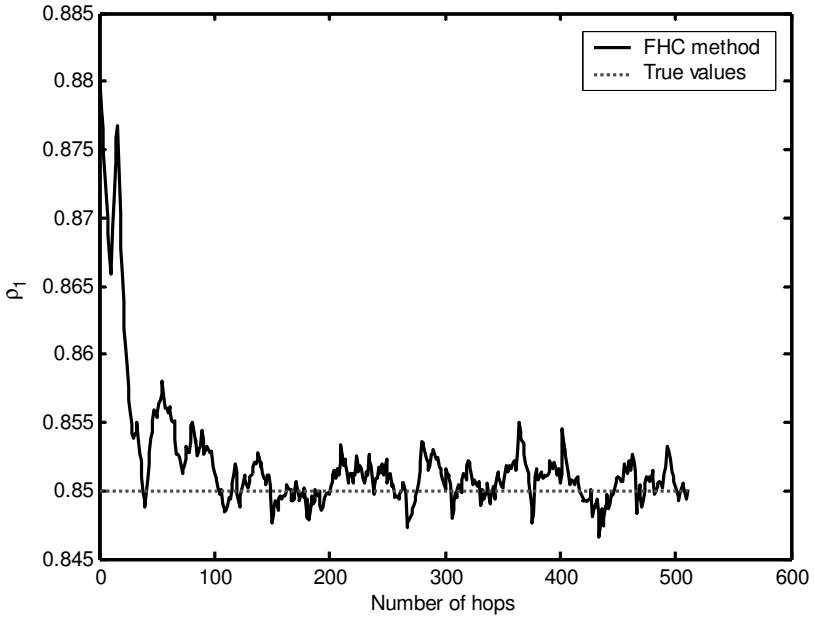

(b) ρ_1 vs. number of hops

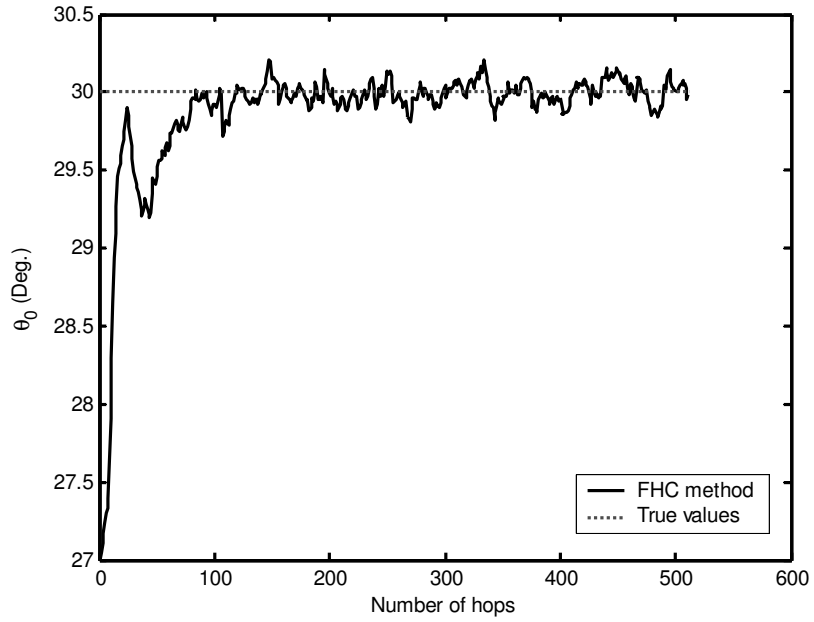

(c) θ_0 vs. number of hops

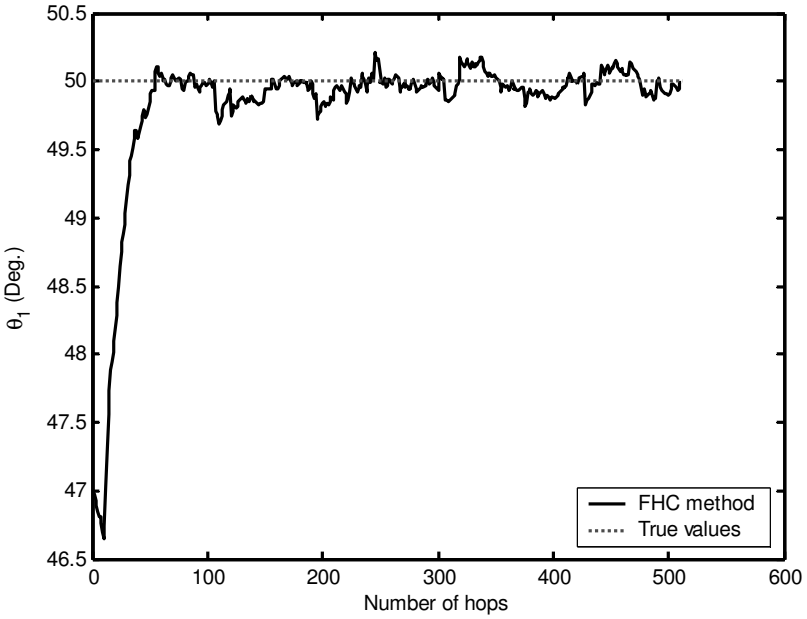

(d) θ_1 vs. number of hops

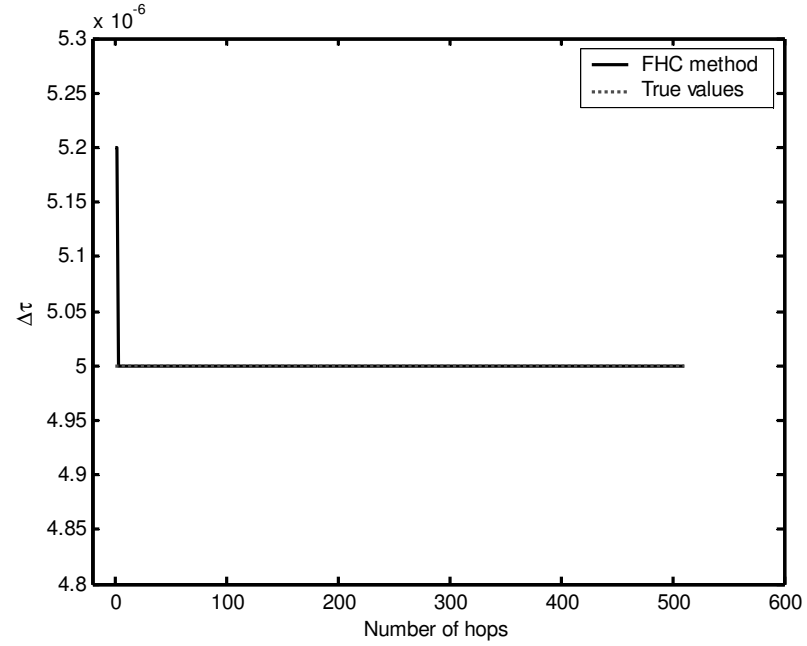

(e) $\Delta\tau$ vs. number of hops

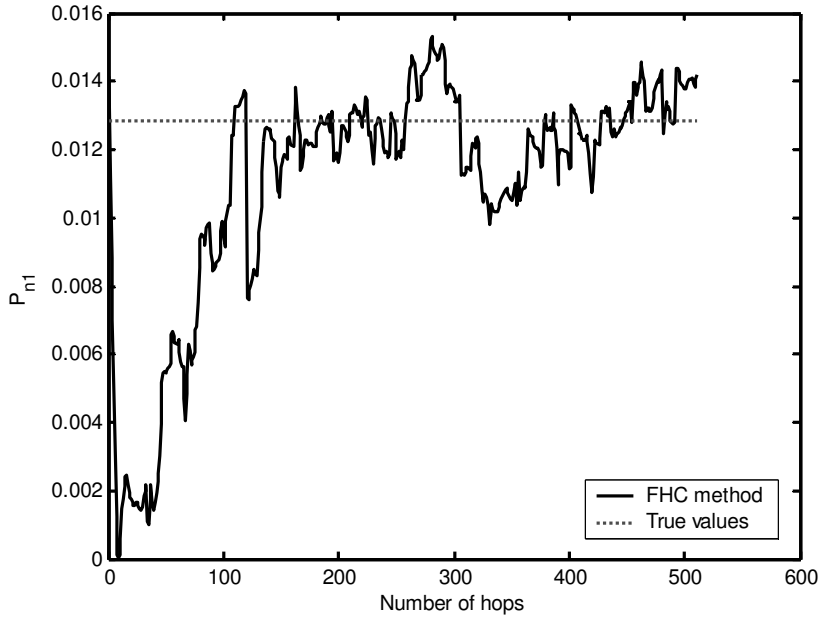

(f) P_{n1} vs. number of hops

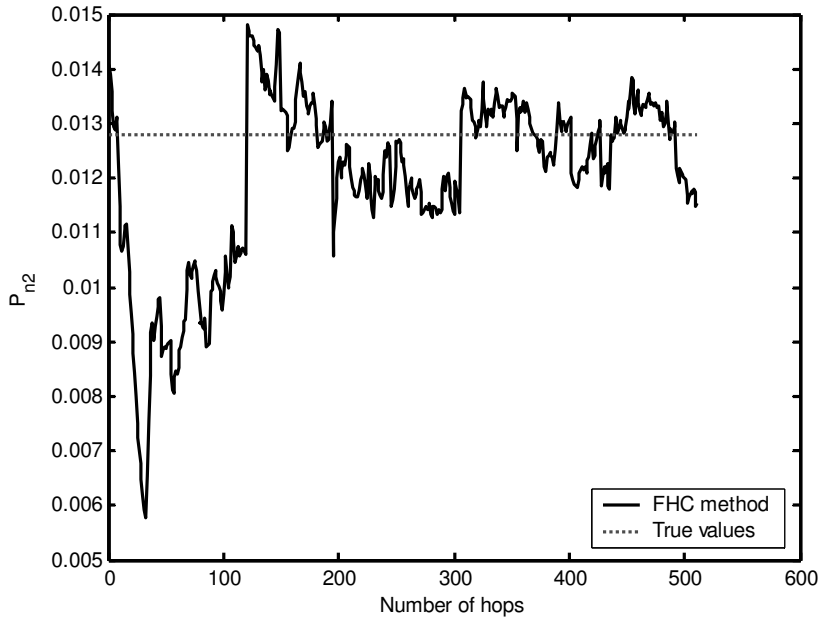

(g) P_{n2} vs. number of hops

Fig. 4.4 Convergence figures of FHC method for Stationary Case

Fig. 4.4 shows the converged parameters of the FHC method in the stationary case when SNR=20dB. The solid lines are iteration results generated by the Gauss-Newton method. The dotted lines are the true values of unknown parameters. We can see the direction parameters converge to their true values after 200 iterations.

4.3 Simulation of Tracking Slow Moving FH signals

In this section, we will present the simulation result of tracking slow moving FH signals. For slow moving FH signals, the directions of received signals change with respect to hop (or time) slowly. Here we assume that the directions are changing as follows

$$\theta_0(h) = 30^\circ + \sin(2\pi h / 500) \tag{4.4}$$

$$\theta_1(h) = 50^\circ + \sin(2\pi h / 350) \tag{4.5}$$

where h is the hop index. Other parameters are fixed and are the same as the stationary case. Because two hops are used to generate one result in our method, the converged value of the direction is between the angle of current hop and the angle of next hop. Since the directions change slowly, this difference may be very small. Thus we can still track the moving directions. Fig. 4.5 is the convergence figures of the FHC method for slow moving FH signals when SNR=20db. The solid lines are the results of the FHC method while the dotted lines are the true values of unknown parameters. It is clear that the iteration results of directions can track the moving directions.

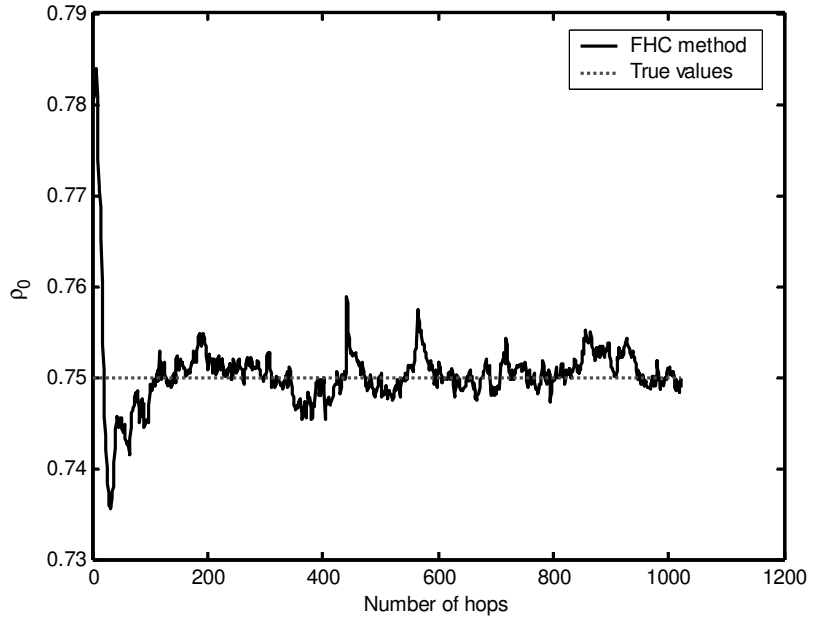

(a) ρ_0 vs. number of hops

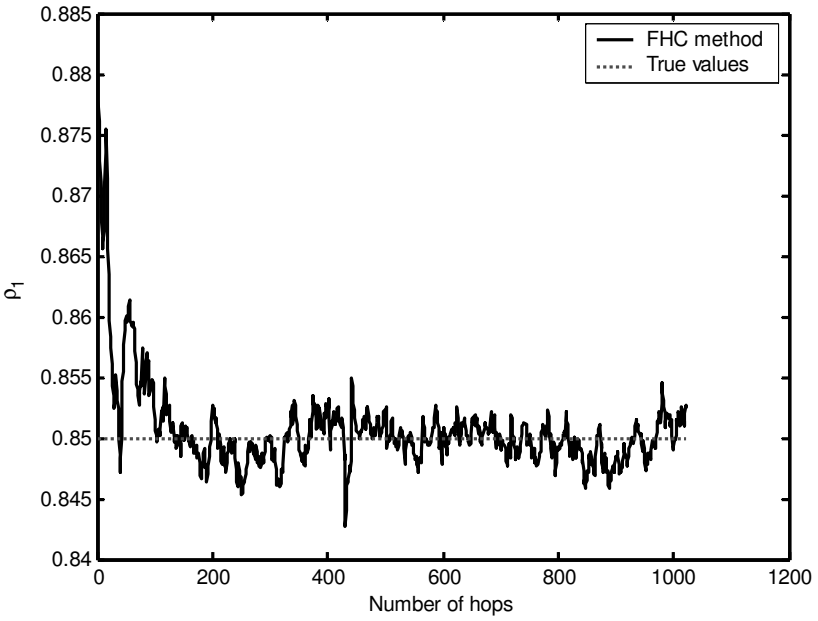

(b) ρ_1 vs. number of hops

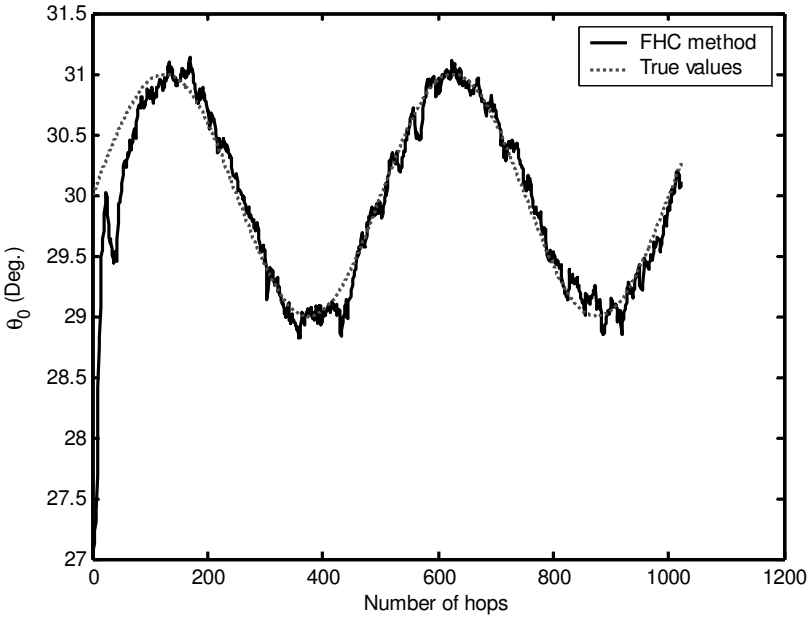

(c) θ_0 vs. number of hops

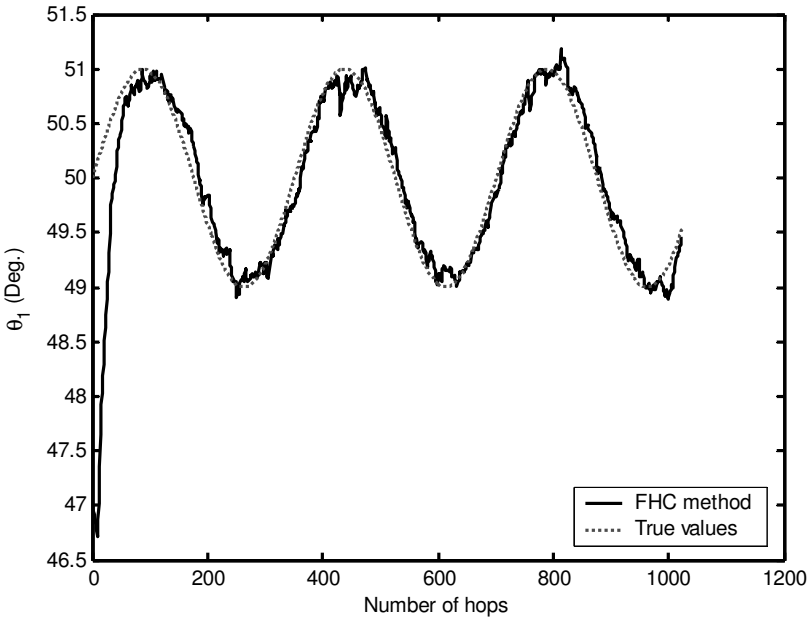

(d) θ_1 vs. number of hops

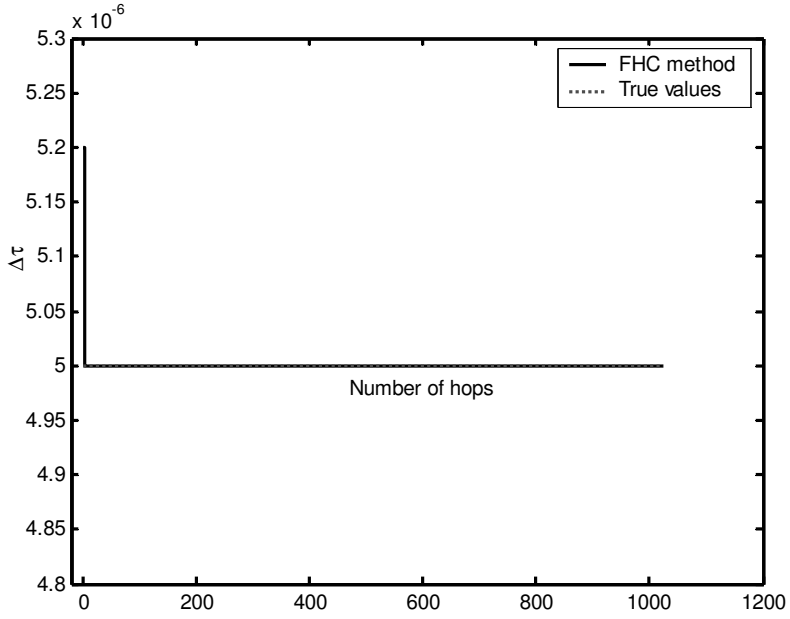

(e) $\Delta\tau$ vs. number of hops

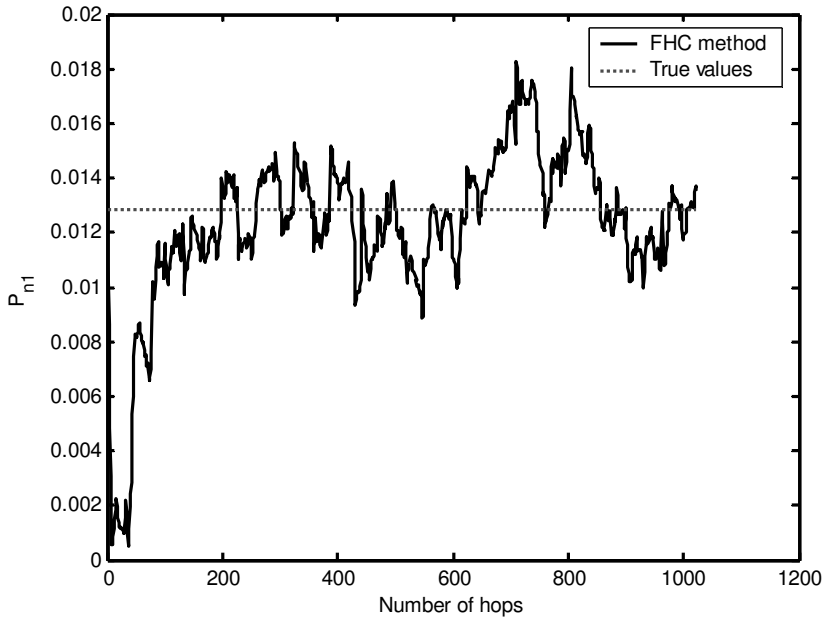

(f) P_{n1} vs. number of hops

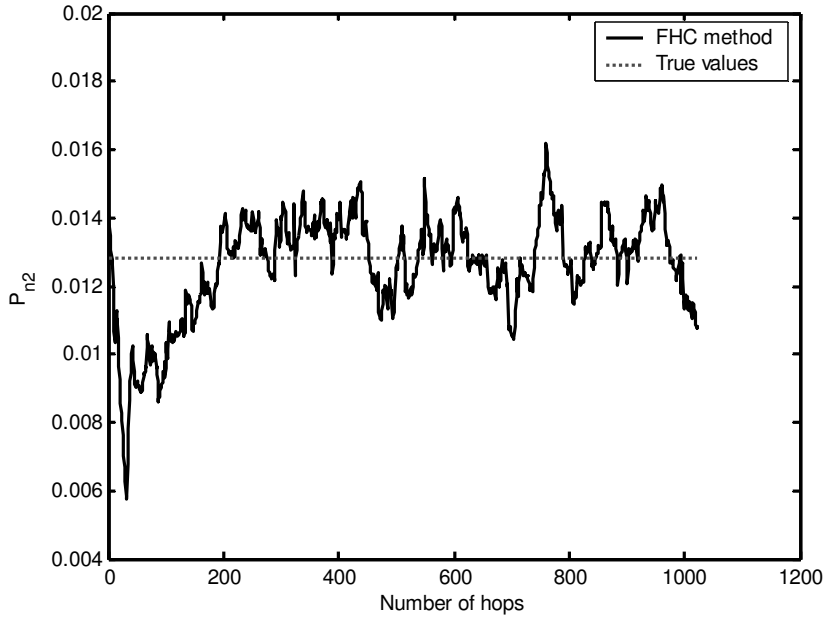

(g) P_{n2} vs. number of hops

Fig. 4.5 Convergence figures of FHC method for Slow Moving Case

4.4 FHML (Frequency Hopping Maximum Likelihood) method

4.4.1 Introduction to the FHML method

The FHML (Frequency Hopping Maximum Likelihood) method [23] is proposed by Zhi *et al*. The idea is to use two contiguous hops to obtain a structure which can apply the maximum likelihood method. In the FHML method, the receiving antenna is also a two-element array. The received signal can be formulated as follows

$$\mathbf{X}(n)=\begin{bmatrix} x_{0h}(n) \\ x_{0h+1}(n) \\ x_{1h}(n) \\ x_{1h+1}(n) \end{bmatrix}=\sum_{p=0}^{P-1} g_p \begin{bmatrix} e^{-j\alpha_h\tau_p}e^{jn\omega_h T_s} \\ e^{-j\alpha_{h+1}\tau_p}e^{jn\omega_{h+1}T_s} \\ e^{-j\alpha_h(\tau_p+\beta_p)}e^{jn\omega_h T_s} \\ e^{-j\alpha_{h+1}(\tau_p+\beta_p)}e^{jn\omega_{h+1}T_s} \end{bmatrix}=\sum_{p=0}^{P-1} g_p \mathbf{D}^n \mathbf{S}_p,\ \ n=0,\cdots,N-1 \quad (4.6)$$

where $\mathbf{S}_p = \left[e^{-j\alpha_h\tau_p} \quad e^{-j\alpha_{h+1}\tau_p} \quad e^{-j\alpha_h(\tau_p+\beta_p)} \quad e^{-j\alpha_{h+1}(\tau_p+\beta_p)}\right]^{\mathrm{T}}$, $\alpha_h = \omega_c + \omega_h$, h is the hop index and

$$\mathbf{D}^n = \begin{bmatrix} e^{jn\omega_h T_s} & 0 & 0 & 0 \\ 0 & e^{jn\omega_{h+1} T_s} & 0 & 0 \\ 0 & 0 & e^{jn\omega_h T_s} & 0 \\ 0 & 0 & 0 & e^{jn\omega_{h+1} T_s} \end{bmatrix}. \tag{4.7}$$

The parameter vector is

$$\boldsymbol{\eta} = \left[\tau_0, \cdots, \tau_{P-1}, \beta_0, \cdots, \beta_{P-1}\right]^{\mathrm{T}} \tag{4.8}$$

Equation (4.6) can be written in the form of

$$\mathbf{X}(n) = \mathbf{D}^n \mathbf{S}(\boldsymbol{\eta})\mathbf{G} \tag{4.9}$$

where $\mathbf{S}(\boldsymbol{\eta}) = \left[\mathbf{S}_0, \cdots, \mathbf{S}_{P-1}\right]$, $\mathbf{G} = \left[g_0, \cdots, g_{P-1}\right]^{\mathrm{T}}$.

In the presence of independent receiver noise, the received signal vector becomes

$$\mathbf{X}(n) = \mathbf{D}^n \mathbf{S}(\boldsymbol{\eta})\mathbf{G} + \mathbf{V}(n) \tag{4.10}$$

where $\mathbf{V}(0), \ldots, \mathbf{V}(N-1)$ are independent noise vectors with zero mean and a covariance vector $\sigma^2\mathbf{I}$. The likelihood function of received signals is

$$f(\boldsymbol{\eta}) = \frac{1}{\left(\sqrt{2\pi}\sigma\right)^{4N}} e^{-\frac{1}{2\sigma^2}\sum_{n=0}^{N-1}\left\|\mathbf{X}(n)-\mathbf{D}^n\mathbf{S}(\eta)\mathbf{G}\right\|^2} \tag{4.11}$$

The unknown parameters can be found by maximizing the likelihood function. From (4.11), this is equivalent to minimizing the objective function

$$\psi(\boldsymbol{\eta}) = \frac{1}{N}\sum_{n=0}^{N-1}\left\|\mathbf{X}(n) - \mathbf{D}^n\mathbf{S}(\boldsymbol{\eta})\mathbf{G}\right\|^2 \tag{4.12}$$

The gradient of $\psi(\boldsymbol{\eta})$ with respect to $\mathbf{G}$ is

$$\nabla_{\mathbf{G}}\psi(\boldsymbol{\eta}) = \frac{2}{N}\sum_{n=0}^{N-1}\mathbf{S}^{\mathrm{H}}(\boldsymbol{\eta})\left[\left(\mathbf{D}^n\right)^{\mathrm{H}}\mathbf{X}(n) - \mathbf{S}(\boldsymbol{\eta})\mathbf{G}\right] \tag{4.13}$$

Let (4.13) be zero, the likelihood estimator for $\mathbf{G}$ is

$$\hat{\mathbf{G}} = \mathbf{S}(\boldsymbol{\eta})^{+}\mathbf{X}_D \tag{4.14}$$

where $\mathbf{S}(\boldsymbol{\eta})^{+} = \left[\mathbf{S}^{\mathrm{H}}(\boldsymbol{\eta})\mathbf{S}(\boldsymbol{\eta})\right]^{-1}\mathbf{S}^{\mathrm{H}}(\boldsymbol{\eta})$ and $\mathbf{X}_D = \frac{1}{N}\sum_{n=0}^{N-1}\left(\mathbf{D}^{n}\right)^{\mathrm{H}}\mathbf{X}(n)$.

Substituting the estimator of $\mathbf{G}$ into (4.12), we have

$$\psi(\boldsymbol{\eta}) = \mathrm{trace}\left[\frac{1}{N}\sum_{n=0}^{N-1}\mathbf{X}(n)\mathbf{X}^{\mathrm{H}}(n) - \mathbf{P}(\boldsymbol{\eta})\mathbf{X}_D{\mathbf{X}_D}^{\mathrm{H}}\right] \tag{4.15}$$

where $\mathbf{P}(\boldsymbol{\eta}) = \mathbf{S}(\boldsymbol{\eta})\mathbf{S}(\boldsymbol{\eta})^{+}$.

The maximum likelihood estimator of $\boldsymbol{\eta}$ is then given by

$$\hat{\boldsymbol{\eta}} = \arg\min_{\boldsymbol{\eta}} \left\| l(\boldsymbol{\eta}) \right\|^2 \tag{4.16}$$

where

$$l(\boldsymbol{\eta}) = \mathbf{P}^{\perp}(\boldsymbol{\eta})\mathbf{X}_D \tag{4.17}$$

$$\mathbf{P}^{\perp}(\boldsymbol{\eta}) = \mathbf{I} - \mathbf{P}(\boldsymbol{\eta}). \tag{4.18}$$

The solution for $\hat{\boldsymbol{\eta}}$ can be obtained by applying Gauss-Newton method

$$\hat{\boldsymbol{\eta}}(k+1) = \hat{\boldsymbol{\eta}}(k) - \mu \cdot \left\{\nabla_{\hat{\boldsymbol{\eta}}(k)} \left\| l[\hat{\boldsymbol{\eta}}(k)] \right\|^2\right\}^{+} \cdot \left\| l[\hat{\boldsymbol{\eta}}(k)] \right\|^2 \tag{4.19}$$

where $\left\{\nabla_{\hat{\boldsymbol{\eta}}(k)} \left\| l[\hat{\boldsymbol{\eta}}(k)] \right\|^2\right\}^{+}$ is Moore-Penrose pseudo-inverse of $\nabla_{\hat{\boldsymbol{\eta}}(k)} \left\| l[\hat{\boldsymbol{\eta}}(k)] \right\|^2$.

The derivative of the objective function is given by

$$\nabla_{\hat{\boldsymbol{\eta}}(k)} \left\| l[\hat{\boldsymbol{\eta}}(k)] \right\|^2 = \frac{\partial \left\| l[\boldsymbol{\eta}(k)] \right\|^2}{\partial \eta_i} = -2\,\mathrm{Re}\left({\mathbf{X}_D}^{\mathrm{H}}{\mathbf{S}^{+}}^{\mathrm{H}}{\dot{\mathbf{S}}_{\eta_i}}^{\mathrm{H}}\mathbf{P}^{\perp}\mathbf{X}_D\right) \tag{4.20}$$

where

$$\dot{\mathbf{S}}_{\eta_i} = \frac{\partial \mathbf{S}}{\partial \eta_i} = \left[\frac{\partial \mathbf{S}_0}{\partial \eta_i}, \cdots, \frac{\partial \mathbf{S}_{P-1}}{\partial \eta_i}\right]. \tag{4.21}$$

4.4.2 Simulation of the FHML method

To compare the FHML method with the FHC method, the simulation scenario of the FHML method is completely same as that of the FHC method. The initial parameters are set at $\boldsymbol{\eta} = \left[5.05\mu s \quad 10.05\mu s \quad 27^\circ \quad 47^\circ\right]^T$. The step size is $\mu = 0.5$. SNR=20dB. Each step of the iteration uses two successive hops to generate one result. Fig. 4.6 and Fig. 4.7 show the algorithm performance in stationary case and slow moving case, respectively.

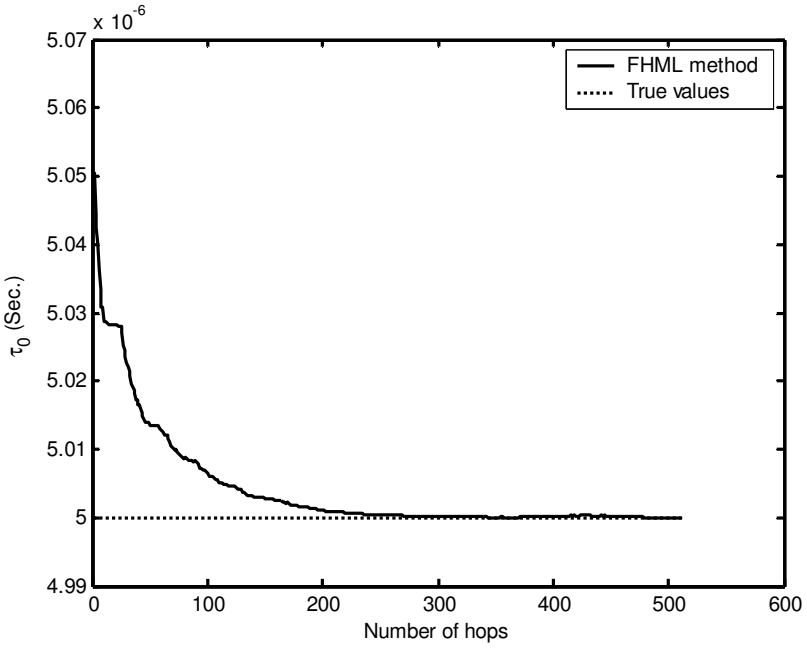

(a) τ_0 vs. number of hops

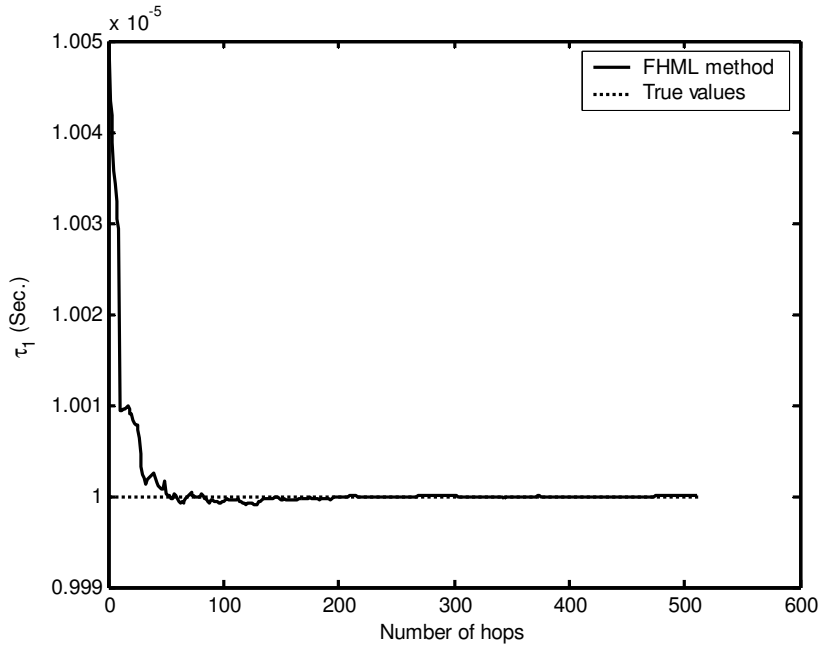

(b) τ_1 vs. number of hops

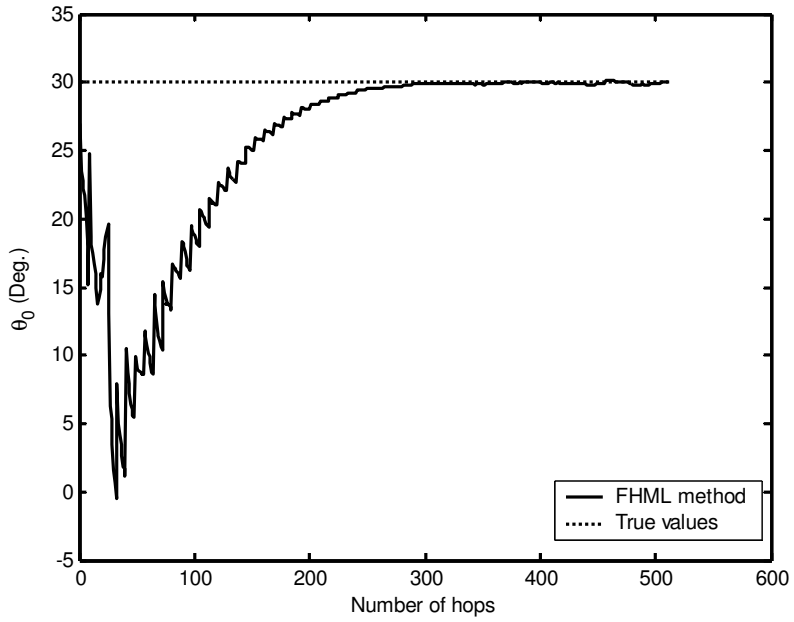

(c) θ_0 vs. number of hops

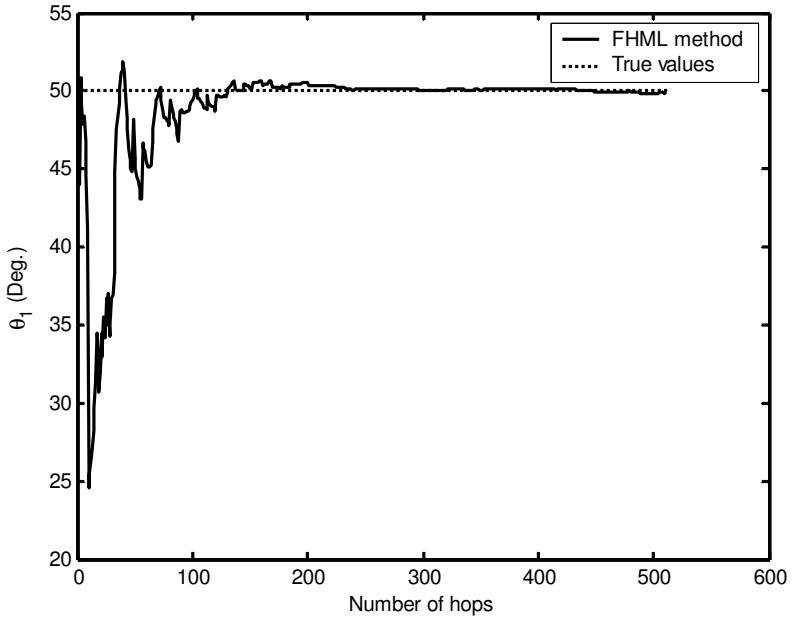

(d) θ_1 vs. number of hops

Fig. 4.6 Convergence figure of stationary case for FHML method.

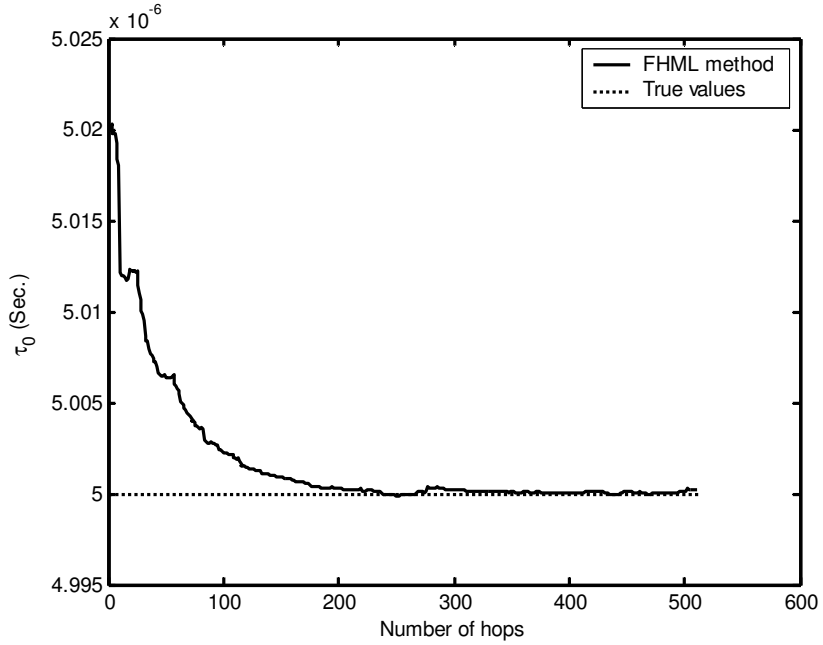

(a) τ_0 vs. number of hops

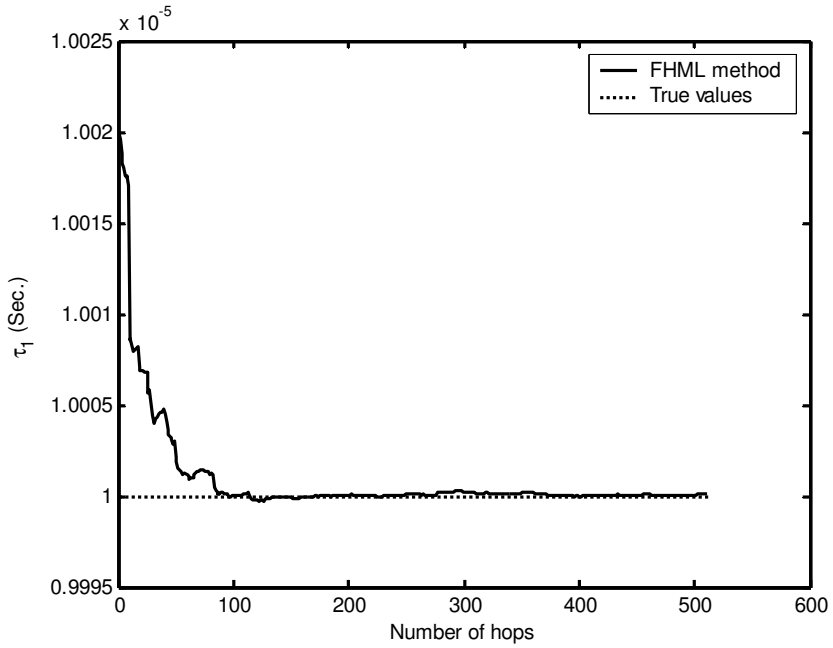

(b) τ_1 vs. number of hops

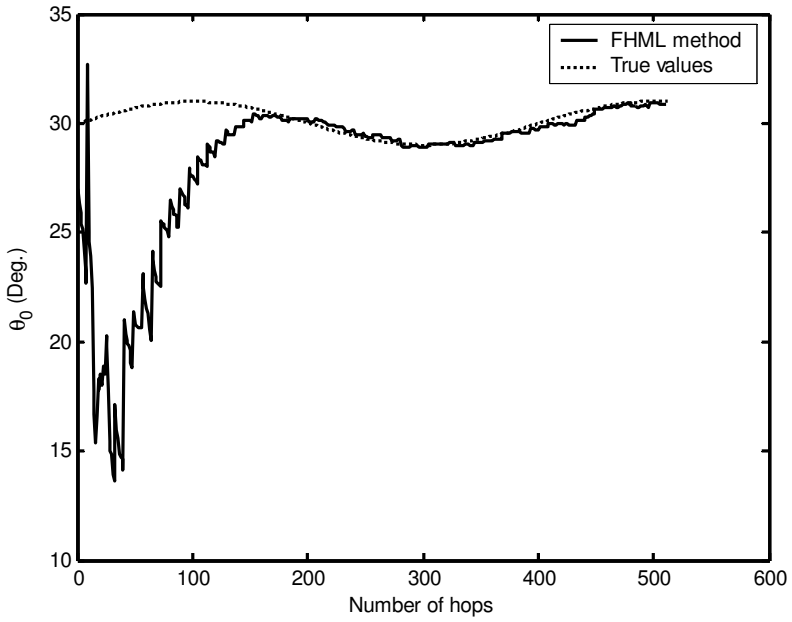

(c) θ_0 vs. number of hops

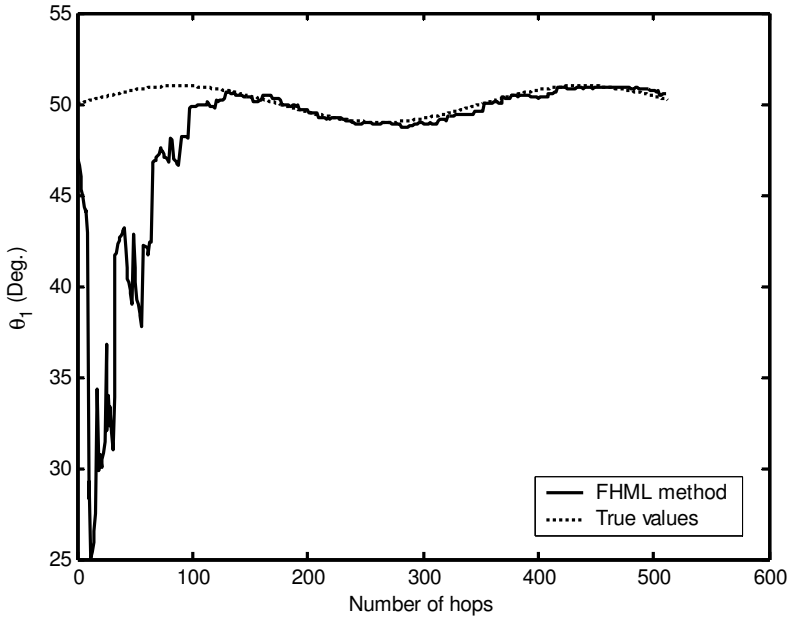

(d) θ_1 vs. number of hops

Fig. 4.7 Convergence figure of slow moving case for FHML method.

It is shown that the FHML method performs well both in estimating directions of stationary FH signals and tracking slow moving FH signals. We will compare the converged results of the FHML method with the FHC method in next section.

4.5 Comparison between FHML method and FHC method

To compare the converged results of the FHML method and the FHC method, the average variances of the angle-of-arrivals θ_0 and θ_1 are measured after they have converged in the stationary case. As shown in Fig. 4.4 and Fig. 4.6, it is obvious that θ_0 and θ_1 converge after 300 iterations. The variances of converged values are calculated from the 350th iteration to the last iteration. Fifty Monte Carlo runs are done and we take the average of the fifty variances for both methods at a given SNR.

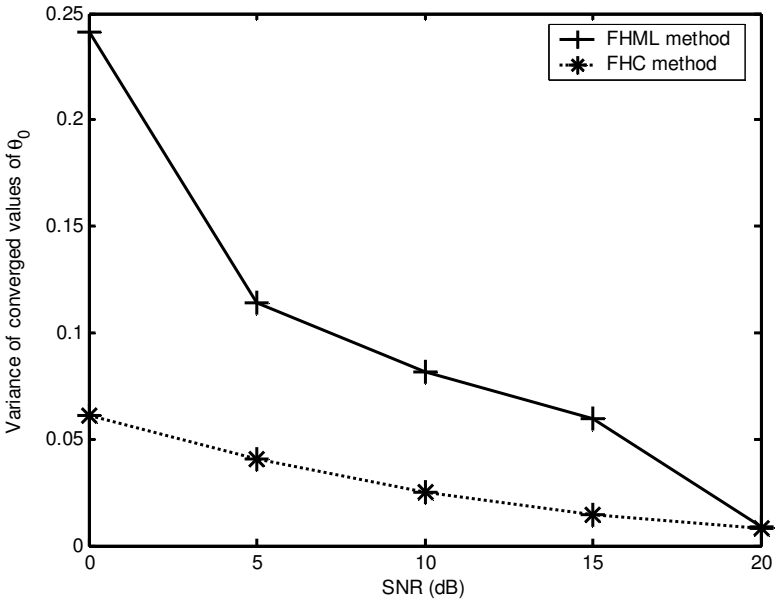

(a) Variances of converged values of θ_0 at different SNR

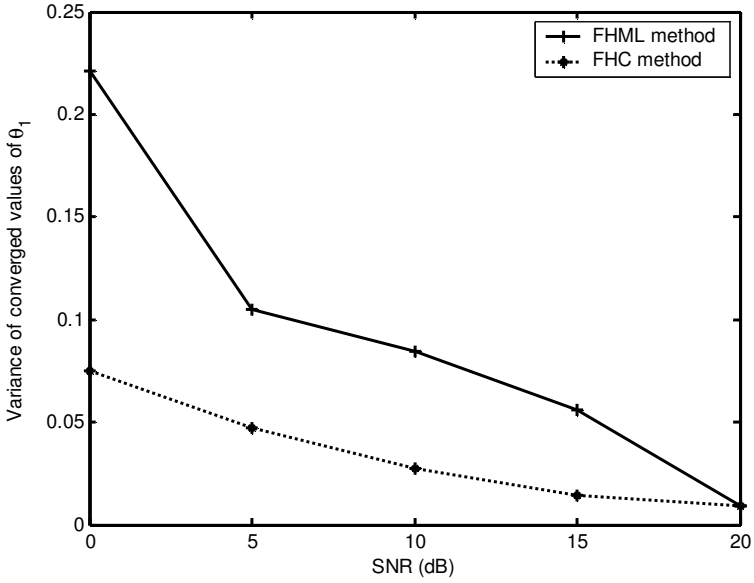

(b) Variances of converged values of θ_1 at different SNR

Fig. 4.8 Variances of converged values of θ vs. SNR.

Fig. 4.8 shows the results at SNR=0dB, 5dB, 10dB, 15dB and 20dB respectively. The asterisk and plus signs denote the average variances of the converged θ at the corresponding SNR. We can see that the variances of converged values for the FHC

method is much smaller than that of the FHML method when SNR is low while they are comparable at SNR=20dB. Thus the converged values of directions of the FHC method are more accurate than that of the FHML method at low SNR.

Other advantages of the FHC method are that only the power of transmitted signal is needed to be known and the correlations of received signal can be measured by analog devices.

4.6 Summary

In this chapter, simulation results of the FHC method are presented, and it is compared with the FHML method. It is shown that the converged results of the new method are more accurate than that of the FHML method. Furthermore, only the power of transmitted signal is needed to be known for the proposed method. The FHC method is easy to implement as analog devices can be used to measure the correlations of received signals.

Chapter 5

Conclusions and Future Work

5.1 Conclusions

Direction finding and DOA estimation are used in various applications. In military communications and some short-range wireless communication systems, frequency hopping techniques are widely used. Some work has already been done to estimate directions for the frequency hopping signals. However, the multipath problem is not considered in these methods. Therefore, in communication systems where multipath propagation exists, these methods may be not effective. Furthermore, a large size antenna array (the number of array elements is larger than the number of signal sources) is needed at the receiver, which is difficult to install on the mobile devices.

In this thesis, the Frequency Hopping Correlation (FHC) method is proposed to solve the problem of direction finding for the frequency hopping signals under multipath propagation using a two-element array. By minimizing the difference between the estimated correlations and the measured correlations of received signals, the objective function is established. Generally, the objective function is highly oscillatory with respect to time delay parameters. Thus a pre-processing is used to obtain re-

fined initial values of the time delays. Then the Gauss-Newton algorithm is used to find the optimum parameters including directions. The simulation results show that the FHC method is effective for both stationary and slow moving frequency hopping signals.

Furthermore, the FHC method is compared with the FHML method. When the Gauss-Newton algorithm is applied to both methods, the converged values of direction parameters of the FHC method are more accurate than those of the FHML method. The new method has another advantage that the correlations can be measured by analog devices.

5.2 Future Work

The FHC method needs to be improved in the following aspects. First, the number of unknown parameters may be reduced so that the Jacobian matrix in the Gauss-Newton method could have a smaller dimension. This is to reduce the computation complexity of the FHC method.

Second, in the slow moving case it is assumed that only the direction parameters change with respect to hops. In practice, other parameters (e.g. time delay) may change with respect to hops or time as well. More analysis can be carried out for this problem in the future.

References

[1] P. H. Lehne and M. Pettersen, "An overview of smart antenna technology for mobile communication systems," IEEE Communications Surveys, vol.2, no. 4, pp.2-13, Fourth Quarter, 1999.

[2] T. S. Rappaport, Wireless communications: Principles & Practice, Chapter 1, Upper Saddle River, NJ: Prentice-Hall, 1996.

[3] T. Biedka *et al*., "Implementation of a prototype smart antenna for low tier PCS," Proc. 49th IEEE VTC'99- Spring, vol.1, pp.448-452, Houston, TX, USA, May 1999.

[4] M.G. Kyeong *et al*., "Outdoor communications using adaptive arrays in CDMA mobile systems," Proc. 49th IEEE VTC'99-Spring, vol.1, pp.264- 268, Houston, TX, USA, May 1999.

[5] S. Tanaka *et al*., "Experiment on coherent adaptive antenna array diversity for wideband CDMA mobile radio," Proc. 49th IEEE VTC'99-Spring, vol.1, pp.243-248, Houston, TX, USA, May 1999.

[6] B. H. Wellenhof *et al*. Global positioning system: theory and practice, Wien, NY: Springer-Verlag, 1997.

[7] T. S. Rappaport, J. H. Reed and B. D. Woerner, "Position location using wireless communication on highways of the future," IEEE Communications Magazine, vol.34, pp.33-41, October 1996.

[8] H. Krim and M. Viberg, "Two decades of array signal processing research," IEEE Signal Processing Magazine, vol.13, pp.67-94, July 1996.

[9] J. G. Proakis, Digital communications, Chapter 13, Boston, McGraw-Hill, 2000.

[10] R. Roy, A. Paulraj and T. Kailath, "ESPRIT- A subspace rotation approach to estimation of parameters of cisoids in noise," IEEE Trans. Acoustics, Speech and Signal Processing, vol. 34, pp.1340-1342, Oct 1986

[11] H. Krim, "A data-based enumeration technique for fully correlated signals," IEEE Trans. Acoustic, Speech and Signal Processing, vol.42, pp.1662-1668, July 1994.

[12] T. J. Shan, M. Wax and T. Kailath, "On spatial smoothing for directions of arrival estimation of coherent signals," IEEE Trans. Acoustics, Speech and Signal Processing, vol.33, pp. 806-811, April 1985.

[13] M. Wax, "Detection and localization of multiple sources in noise with unknown covariance," IEEE Trans. Acoustic, Speech and Signal Processing, vol.40, pp. 245-249, Jan. 1992

[14] B. Friedlander and A. Weiss, "Direction finding using spatial smoothing with interpolated arrays," IEEE Trans. Aerospace and Electronic Systems, vol. 28, pp.574-587, Apr. 1992.

[15] K. T. Wong, "Blind beamforming/geolocation for wideband-FFHs with unknown hop sequence," IEEE Trans. Aerospace and Electronic Systems, vol.37, pp.65-76, Jan. 2001.

[16] Xiangqian Liu, N. D. Sidiropoulos and A. Swami, "Blind high-resolution local-

ization and tracking of multiple frequency hopped signals," IEEE Trans. Signal Processing, vol. 50, pp.889-901, Apr. 2002.

[17] The official Bluetooth membership site, "Bluetooth core specification." http://www.bluetooth.org/spec/

[18] P. D. Rasky *et al*, "Slow frequency-hop TDMA/CDMA for macrocellular personal communications," IEEE Personal Communications, vol.1, pp. 26-35, 2nd quarter, 1994.

[19] B. Farhang-Boroujeny, Adaptive filters: Theory and Applications, Chapter 5. West Sussex, England, John Wiley & Sons Ltd, 2000.

[20] M. S. Bazaraa, H. D. Sherali and C. M. Shetty, Nonlinear Programming: Theory and Algorithm, Chapter 8. John Wiley & Sons, Inc, 1993.

[21] I. Ziskind and M. Wax, "Maximum likelihood localization of multiple sources by alternating projection," IEEE Trans. Acoustics, Speech and Signal Processing, vol. 36, pp.1553-1560, Oct. 1988.

[22] X. Li, E. G. Larsson, M. Sheplak and J. Li, "Phase-shift-based time-delay estimators for proximity acoustic sensors," IEEE Journal of Oceanic Engineering, vol. 27, pp.47-56, Jan. 2002.

[23] Wanjun Zhi, Francois Chin and C. C. Ko, "Multi-hop ML Based Delay and Angle Estimation for Multipath Wideband Frequency Hopping Signals," Proc. IEEE VTC'04-Spring, Milan, Italy, May 2004.

[24] C. C. Ko and C. S. Siddharth, "Rejection and tracking of an unknown broadband source in a two-element array through least square approximation of in-

ter-element delay," IEEE Signal Processing Letters, vol.6, pp.122-125, May 1999.

[25] P. Stoica and K. C. Sharman, "Maximum likelihood methods for direction-of-arrival estimation," IEEE Trans. Acoustics, Speech and Signal Processing, vol. 38, pp.1132-1143, Jul. 1990.

[26] T. G. Manickam, R. J. Vaccaro and D. W. Tufts, "A least squares algorithm for multipath time-delay estimation," IEEE Trans. Signal Processing, vol. 42, pp.3229-3233, Nov. 1994.

[27] L. C. Godara, "Applications of antenna arrays to mobile communications, Part I: performance improvement, feasibility, and system considerations," Proceedings of the IEEE, vol. 85, pp.1031-1060, July 1997

[28] L. C. Godara, "Applications of antenna arrays to mobile communications, Part II: beamforming and direction-of-arrival considerations," Proceedings of the IEEE, vol. 85, pp.1195-1245, Aug. 1997

[29] J. J. Fuchs, "Multipath time-delay detection and estimation," IEEE Trans. Signal Processing, vol. 47, pp.237-243, Jan. 1999